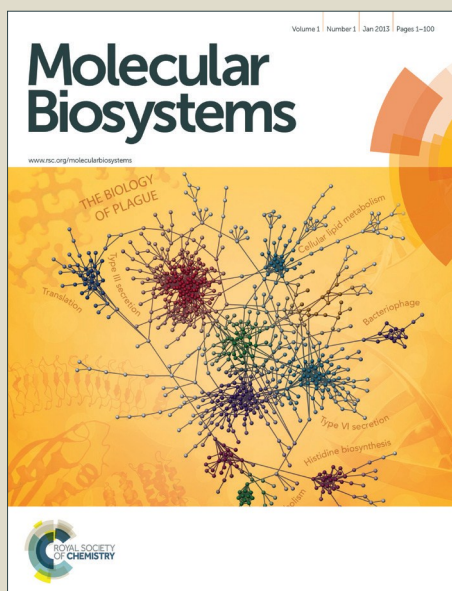


Molecular BioSystems

Accepted Manuscript



This is an *Accepted Manuscript*, which has been through the Royal Society of Chemistry peer review process and has been accepted for publication.

Accepted Manuscripts are published online shortly after acceptance, before technical editing, formatting and proof reading. Using this free service, authors can make their results available to the community, in citable form, before we publish the edited article. We will replace this *Accepted Manuscript* with the edited and formatted *Advance Article* as soon as it is available.

You can find more information about *Accepted Manuscripts* in the [Information for Authors](#).

Please note that technical editing may introduce minor changes to the text and/or graphics, which may alter content. The journal's standard [Terms & Conditions](#) and the [Ethical guidelines](#) still apply. In no event shall the Royal Society of Chemistry be held responsible for any errors or omissions in this *Accepted Manuscript* or any consequences arising from the use of any information it contains.



www.rsc.org/molecularbiosystems

Metabolomic Analysis of Survival in Carbohydrate Pre-fed Pigs Subjected to Shock and Polytrauma

Nancy E Witowski¹, Elizabeth R Luszczek¹, Charles E Determan Jr¹, Daniel R Lexcen¹, Kristine E Mulier¹, Andrea Wolf¹, Beverly G Ostrowski², Greg J Beilman¹

¹ Department of Surgery, University of Minnesota, Minneapolis, MN

² Minnesota NMR Center, University of Minnesota, Minneapolis, MN

Abstract:

Hemorrhagic shock, a result of extensive blood loss, is a dominant factor in battlefield morbidity and mortality. Early rodent studies in hemorrhagic shock reported carbohydrate feeding prior to the induction of hemorrhagic shock decreased mortality. When repeated in our laboratory with a porcine model, carbohydrate pre-feed resulted in a 60% increase in death rate following hemorrhagic shock with trauma when compared to fasted animals (15/32 or 47% vs 9/32 or 28%). In an attempt to explain the unexpected death rate for pre-fed animals, we further investigated the metabolic profiles of pre-fed non-survivors (n = 15) across 4 compartments (liver, muscle, serum, and urine) at specific time intervals (pre-shock, shock, and resuscitation) and compared them to pre-fed survivors (n = 17). As hypothesized, pre-fed pigs that died as a result of hemorrhage and trauma showed differences in their metabolic and physiologic profiles at all time intervals and in all compartments when compared to pre-fed survivors. Our data suggest that, although all animals were subjected to the same shock and trauma protocol, non-survivors exhibited altered carbohydrate processing as early as the pre-shock sampling point. This was evident in (for example) the higher levels of ATP and markers of greater anabolic activity in the muscle at the pre-shock time point. Based on the metabolic findings, we propose two mechanisms that connect pre-fed status to a higher death rate: 1) animals that die are more susceptible to opening of the mitochondrial permeability transition pore, a major factor in ischemia/reperfusion injury; and 2) loss of fasting-associated survival mechanisms in pre-fed animals.

Table of contents: Metabolomics data from four compartments in porcine polytrauma suggest differences in carbohydrate processing between survivors and non-survivors even before injury.

1. Introduction

Hemorrhagic shock is the pathophysiologic state that accompanies extensive blood loss and remains a dominant factor in battlefield morbidity and mortality¹. The response to trauma is

complex², with several predictive models of outcome and severity of injury studied³⁻⁵. One such predictor is pre-trauma state. Unsurprisingly, pre-existing disease negatively impacts outcomes in trauma patients⁶. Alternatively, pre-injury state may be leveraged to improve outcomes. Studies in rodents report higher survival rates associated with carbohydrate feeding prior to the induction of hemorrhagic shock⁷⁻⁹.

We have previously reported that the metabolic as well as the physiologic profiles in pre-fed animals differed from that of fasted animals in a porcine model of hemorrhagic shock with injury and resuscitation¹⁰⁻¹³. In this study, both fasted and pre-fed pigs were allowed water *ad libitum* during an overnight fast. The pre-fed group then received an oral bolus of carbohydrate solution one hour prior to surgery. Contrary to previous reports in rodent models⁷⁻⁹, the death rate for pre-fed animals in our study was nearly double that of fasted animals (15/32 or 47% vs 9/32 or 28%)¹⁰.

In an attempt to explain the unexpected death rate for pre-fed animals, we further analyzed the metabolic and physiologic profiles of pre-fed non-survivors and pre-fed survivors from our original experiment¹⁰⁻¹³. We hypothesized that non-survivors would exhibit profiles that differed from survivors. In this report we present the metabolic and physiologic profiles associated with outcome in the pre-fed group across 4 compartments (liver, muscle, serum, and urine) at specific time intervals: pre-shock, shock, and resuscitation. As hypothesized we found that pre-fed pigs that died as a result of hemorrhage and trauma showed differences in their metabolic and physiologic profiles in all time intervals. Based on these findings, we propose two mechanisms that connect pre-fed status to a higher death rate: 1) animals that die are more susceptible to opening of the mitochondrial permeability transition pore, a major factor in ischemia/reperfusion injury; and 2) loss of fasting-associated survival mechanisms in pre-fed animals.

2. Methods

2.1 Animal Preparation and Hemorrhagic Shock Protocol

The experimental protocol was approved by the University of Minnesota Institutional Animal Care and Use Committee and was conducted in accordance with established guidelines for the treatment of laboratory animals. A modification of our well-established model of porcine hemorrhagic shock^{14,15} was used as described in previous work^{10,12,13} (**Fig. 1**). In short, for the pre-fed group, 32 Yorkshire pigs (Manthei Hog Farm, LLC, Elk River, MN) weighing between 15-20 kg were fasted overnight but allowed free access to water for 12 hours prior to the execution of the protocol. Animals were given an oral carbohydrate solution (Karo Light[®], 7cc/kg, diluted with an equal volume of water) 60 minutes prior to the administration of initial anesthesia. [¹H NMR of Karo Light[®] indicated it is a mixture of mono- and di-saccharides (glucose, fructose, maltose, sucrose)].

Animals were anesthetized, intubated and ventilated to maintain a PaO₂ of 70-120 torr and a PaCO₂ of 35-45 torr (SERVO Ventilator 900C, Siemens, Malvern, PA). After surgical preparation, animals were allowed to stabilize until plasma lactate levels reach a value of 2.0 mmol/L or less, at which time Baseline (B) measurements were taken.

Pigs were exposed to a blunt percussive chest injury, hemorrhage by withdrawal of blood from the inferior vena cava to a systolic blood pressure <60mm Hg, and a liver crush injury using a Holcomb clamp¹⁶. 45 minutes after the start of shock induction, animals were resuscitated with boluses of lactated Ringer's solution during the first hour, and boluses of lactated Ringer's solution and shed blood during the next 20 hours of resuscitation (for the detailed resuscitation protocol see Colling et al.¹⁰). Pigs were extubated after 20 hours of full resuscitation. 48 hours after the end of resuscitation, animals were re-intubated for endpoint sample harvesting and then euthanized with intravenous Beuthanasia D (1 ml/10kg).

Physiologic and oxygen parameters were analyzed as described in Colling et al¹⁰.

2.2 Sampling for Metabolomic Analysis

Serum, urine and tissue (muscle and liver) samples were collected at Baseline (B), 45 minutes after the beginning of the shock period (S45) and two hours after the advent of full resuscitation (FR2). Samples were stored at -80 °C until analysis.

2.3 Nuclear Magnetic Resonance Spectroscopy (NMR)

2.3.1 NMR Spectroscopy of Tissue Samples. Muscle and liver samples were processed for NMR analysis according to established protocol¹⁷. Frozen biopsy specimens were pulverized to a fine powder using a liquid nitrogen-chilled mortar and pestle. Ice-cold perchloric acid (6%, 5 mL/g wet weight) was added to the pulverized tissue (100-150 mg wet weight), and the sample vortexed for 30 seconds. Following a 10 minute incubation on ice, samples were centrifuged (14,000 rpm, 4° C), the pH of the supernatants adjusted to between 7 and 8 with 2M K₂CO₃ and the neutralized samples incubated on ice for 30 min. The KClO₄ precipitate was removed by centrifugation. The resulting supernatant was lyophilized (LABCONCO Freezone 6 plus freeze-dryer, Kansas City, MO) and stored at -80 °C until NMR analysis.

Lyophilized samples were reconstituted in 500 µl D₂O (99.9%; Sigma-Aldrich, St. Louis, MO); 50 µl of 3 mM 2,2-dimethyl-2-silapentane-5-sulfonate (DSS, Cambridge Labs) was added to serve as a lock signal and chemical shift reference ($\delta = 0.0$). Solution pH was adjusted with DCl and NaOD to 7.4. The final volume was brought to 600 µL with D₂O making the solution 0.25 mM in DSS and the sample was transferred to a 5mm NMR tube (Wilmad, Vineland, NJ).

^1H NMR data acquisition was performed at 600 MHz using a Varian spectrometer with a 5mm HCN triple resonance probe at 25 °C. Muscle and liver spectra were generated from 128 scans with a basic ^1H acquisition protocol consisting of a 45° tip angle, a relaxation delay of 1 sec and an acquisition time of 7 sec. A spectral width of 8,000 Hz was used. Phases and baselines were corrected manually before integration. Chemical shifts were assigned relative to the internal standard signal at 0 ppm.

2.3.2 NMR Spectroscopy of Serum Samples. Five hundred μL of thawed serum were mixed with 50 μL of 1 mM trimethylsilylpropionic acid (TSP, Sigma-Aldrich, St. Louis, MO). (TSP served as a lock signal and chemical shift reference ($\delta = 0.0$). Sample pH measured ~ 8 and was not further adjusted. The sample was transferred to a 5mm NMR tube ¹⁸.

One-dimensional ^1H -NMR spectra were acquired on a 700-MHz Bruker Avance NMR spectrometer with a 5-mm TXI proton-enhanced cryoprobe. A Carr-Purcell-Meiboom-Gill presaturation pulse sequence with a spectral width of 10 kHz was used to acquire all spectra with 128 scans and an acquisition time of 3 sec, which were subsequently phase and baseline corrected ¹⁸. Chemical shifts were assigned relative to the internal standard signal at 0 ppm.

2.3.3 NMR Spectroscopy of Urine Samples. One mL of thawed urine was mixed with 0.5 mL of 0.2 M sodium phosphate buffer. The solution was placed on ice for 10 min and then centrifuged at 7000 $\times g$ for 10 min. Five hundred μL of the supernatant were withdrawn and combined with 50 μL of 1 mM TSP, which served as a lock signal and chemical shift references ($\delta = 0.0$) ¹⁹. The pH of the final solution was recorded and the mixture was transferred to a 5 mm NMR tube.

Proton NMR spectra were taken with a 700 MHz Bruker Avance spectrometer with autosampler and 5 mm triple resonance $^1\text{H}/^{13}\text{C}/^{15}\text{N}$ TXI CryoProbe with Z-gradient, running TopSpin v. 2.16 (Bruker BioSpin, Fremont, CA USA). A 1D Nuclear Overhauser Effect Spectroscopy (NOESY) pulse sequence was used to collect spectra of each sample. The 90° pulse width was calibrated for each sample, and was generally 12–13 μs . The relaxation delay was 2 s, the acquisition time was 3 s, the spectral width was 10 kHz, the total number of data points collected was 63,000, and the number of transients collected was 128, for a total experiment time of 11 min and 17 s. During the relaxation period, the water resonance was presaturated. All spectra were collected at a temperature of 298 K. Line broadening at 0.5 Hz was applied before fast Fourier transform; autophasing and auto-baseline correction were applied by TopSpin.

2.3.4 Spectral Profiling and Quantification. Spectra from each compartment were fit using Chenomx NMR Suite version 7.0 (Edmonton, Alberta, Canada) ²⁰. Fine manual phasing and baseline corrections were applied to each spectrum before targeted profiling was performed. The

identification and assignment of all metabolites was based on chemical shift relative to the designated internal standard and comparison with the published literature including the spectral libraries available in Chenomx and the Human Metabolome Database (www.hmdb.ca). Tissue metabolites (n= 51 in the liver; n= 39 in the muscle) are reported as mM/1 g lyophilized tissue. Serum metabolites (n=53) are reported in mM. Urine metabolite concentrations (n=60) were multiplied by urine output (cc/hour/kg) to correct for changes in the concentration of urine throughout the experiment²¹. The final metabolite abundances (nmol/h/kg) were log-transformed (base 10) to allow for comparisons among metabolites over several orders of magnitude (range: $0-5.9 \times 10^5$ nmol/h/kg). To address taking the logarithm of zero, 0.1 was added to the normalized data. The range of the log-transformed, normalized data was [-1, 5.77]. Urea was removed from the data set because its signal is compromised by the NOESY pulse sequence.

2.4 Statistical Analysis

A multivariate approach was used for data analysis to determine the response to shock. In addition to comparing baseline levels, changes during early time intervals were examined by analyzing differences between each subsequent time point (baseline data were subtracted from S45 data, S45-B; early resuscitation data were subtracted from S45 data, FR2-S45). For urine, only data at a given time point were considered. This was done because urine data normalized to urine output already reflects metabolite abundances over the course of the hour urine was collected. All statistical analysis was conducted in the open source R statistical program v 2.9²² and SPSS (version 22 for Macintosh, IBM Corp, Armonk, NY). For each time point/interval, the profiled metabolites were auto-scaled and mean-centered, and subsequently analyzed by Partial Least Squares Discriminant Analysis (PLS-DA), a common discrimination technique utilized in metabolomics²³⁻²⁵ that has been successfully implemented previously in our lab^{26,27}. The R packages *Discriminer*²⁸ and *permute*²⁹ were used collectively to conduct the PLS-DA model, cross-validation, and permutation tests. PLS-DA models were optimized on the number of misclassifications (NMC)³⁰. Cross-validation (CV) was conducted via cross-model validation, i.e. nested CV, double CV³¹ wherein the dataset was randomly split into training and testing datasets (75%, 25%). PLS-DA models were then generated from the training dataset and a leave-10-out internal cross-validation. Optimized models were then used to predict the testing set (outer cross-validation). Prediction accuracy was calculated from the resulting confusion matrix. Accuracy $\geq 85\%$ and $R^2 \geq 0.500$ were considered potentially useful models. Model quality was assessed by random permutation of group class with 1000 iterations where a low permutation p-value (≤ 0.05) indicated a strong model. Variable importance of projection (VIP) scores were generated for each metabolite. Oxygen and urea data were evaluated for statistical significance by Mann Whitney U test.

3.0 Results

3.1 Model Analysis

Diagnostics for PLS-DA models were created to evaluate models that discriminate outcomes (lived vs died) for each of the liver, muscle, and serum at baseline and early time periods (B, S45-B, FR2-S45; **Table 1**). As stated above, urine models were constructed with single time point data (B, S45, FR2). Two hours after the advent of full resuscitation, all but six of the non-surviving animals had died (**Fig. 2**). As a result, metabolomic data at later time points were not evaluated. According to the criteria stated in the Statistical Analysis section, liver, serum, and urine models at baseline were potentially discriminatory. During the S45-B time interval, liver and serum models were potentially discriminatory. During the FR2-S45 time interval, models for liver, muscle, and serum were potentially discriminatory. Only urine at baseline and urine at S45 met the criteria for strong predictive power ($p \leq 0.05$). The baseline serum model ($p = 0.06$) and the liver and muscle models at FR2-S45 were nearly predictive with $p \leq 0.10$.

Scores plots of PLS-DA models discriminating animals that die from animals that live for each compartment during the response to shock are shown in **Fig 3**. The scores plots for baseline and early resuscitation time intervals are reported in Supplemental Figures 1a and 1b. Identified metabolites are listed for each compartment along with corresponding VIP scores in **Supplemental Table 1**.

3.2 Metabolite Selection

Metabolomics papers commonly present results based on VIP values of descending magnitude with arbitrary cut-offs. In this analysis there are over 150 metabolites arising from the combination of four physiologic compartments with the potential for each profile to be unique to each of the three sampling points. Because this is a study of fuel availability, we opted to report average metabolite levels with an emphasis on fuel source mobilization and processing: 1) glucose and its anaerobic metabolite lactate; 2) amino acids, particularly the branched-chain amino acids isoleucine, leucine, and valine; 3) muscle creatine phosphate (CrP); 4) glycerol as well as the ketone bodies β -hydroxybutyrate and acetoacetate; and 5) ATP. Heat maps profile the patterns of metabolites related to energy use across the early course of the experiment (**Fig. 4**). Following this summary, we list other metabolites that differentiate survival outcomes. In each Results subsection the VIP score (immediately following the metabolite in parentheses) indicates the significance of each metabolite to outcome. In our analysis, scores above one are considered to indicate metabolites that are strongly differentiating between outcomes. When relevant, selected metabolites with lower VIP scores are also reported in the results.

3.3 Baseline (Fig. 5)

Liver: Baseline liver data exhibited lower levels of fuel metabolites in animals that died relative to those that lived. A lower level of pentose phosphate pathway activity is suggested for non-survivors compared to survivors.

Glucose (1.04) and lactate (0.20) levels were lower in animals that died. Levels of branched-chain amino acids (< 0.3) were not differentiating between groups. Levels of several other amino acids [alanine, aspartate, glutamate, glutamine, glycine, serine and the essential amino acids lysine and methionine (>0.8)] were lower in the liver of non-survivors. The level of β -hydroxybutyrate was similar between groups (0.37). In the liver of animals that died the level of ATP (1.61) was lower.

According to the experimental protocol, three to four hours transpire between pre-feeding and baseline sampling. This interval prompted us to examine the downstream results of glucose metabolism. Upon entering the liver cell, glucose is converted to glucose-6-phosphate (G6P). Depending on physiologic conditions G6P can be channeled into different pathways: 1) It can function as fuel source for ATP production; 2) it can be used as a substrate for the pentose phosphate pathway; and 3) it can be converted to glycogen.

When used as a fuel source, glucose is metabolized to pyruvate and then acetyl-CoA, which enters the tricarboxylic acid (TCA) cycle. The electron donors produced by operation of the TCA cycle feed the mitochondrial electron transport chain producing ATP. Lower levels of pyruvate (0.68) and some TCA cycle intermediates [fumarate (0.71), succinate (0.92)] could indicate a reduced level of activity in the TCA cycle in non-survivors. The observed lower level of ATP in non-survivors supports this speculation.

Processing of G6P through the pentose phosphate pathway generates NADPH providing reducing power for biosynthesis and the reduction of oxidized glutathione. G6P can also be converted into ribose-5-phosphate, a building block for purines and pyrimidines (**Fig. 6**). There are indications that the pentose phosphate pathway was active to a lesser degree in non-survivors. The level of reduced glutathione (GSH, 1.09) was decreased in non-survivors. The level of AMP (1.23), a biosynthetic product of ribose-5-phosphate (**Fig. 6**), was lower in non-survivors. Furthermore, pigs that died exhibited decreased levels of hypoxanthine (2.16), a degradation product of AMP. These observations support the hypothesis that non-survivors engage the pentose phosphate pathway to a lesser degree at baseline.

The enzyme phosphoglucomutase converts glucose-6-phosphate to glucose-1-phosphate, a precursor to the growing glycogen polymer. Sufficient glycogen data to evaluate the premise that G6P is preferentially channeled to glycogen production in non-survivors is unavailable. However, glucose information during the shock interval (see Results: Shock - Liver) supports the concept that non-survivors produced more glycogen than did survivors. A potential corollary to this concept is the idea that non-survivors may have processed more glucose than did survivors.

Muscle: Non-glycolytic fuel sources and ATP levels were higher in the muscle of animals that died. Elevated anabolic activity is suggested in non-survivors.

Muscle glucose (0.48) and lactate levels (0.29) trended higher in non-survivors but did not differentiate outcomes. Despite similar glucose availability, levels of the branched-chain amino acids and the degradation product of leucine (3-hydroxyisovalerate) (>1) were higher in non-survivors relative to survivors. With the exception of glycine (1.06), levels of other NMR-visible amino acids [alanine, glutamate, glutamine (< 0.4)] did not differentiate lived from died. The level of CrP (0.40) was similar between outcome groups. The level of β -hydroxybutyrate (1.19) was higher in non-survivors. The level of muscle ATP (1.39) was higher at baseline in animals that died compared to those that lived.

Glucose levels did not differentiate outcome in the muscle at this sampling point. Similar to the liver, we looked downstream for the effects of the carbohydrate pre-feed to be observed. A potential downstream effect of the carbohydrate pre-feed is elevated anabolic activity³². Biosynthetic reactions often require a 1-carbon unit such as formate. Catabolism of tryptophan (not NMR-visible in the muscle; see Urine Results) generates formate and ultimately niacinamide, a precursor for NAD^+ ³³. The levels of formate (1.06), niacinamide (0.45) and NAD^+ (0.85) were higher in non-survivors. Additionally, leucine is recognized as a potent stimulator of protein synthesis^{34,35} and non-survivors exhibited greater levels of leucine (1.29) than did survivors. These combined observations suggest a greater degree of anabolic activity in non-survivors relative to survivors.

Another potential downstream effect of the carbohydrate pre-feed is ATP production. Following glycolytic processing of carbohydrate pre-feed, the resulting metabolites enter the TCA cycle. Operation of the TCA cycle generates NADH and FADH_2 that provide the electron transport chain with electrons used in the oxidative production of ATP. The level of ATP was higher in the muscle of non-survivors compared to survivors. If more carbohydrate is processed through the TCA cycle (arising either from a more efficient oral uptake or a greater cellular ability to process carbohydrate), then more ATP is produced. The level of glucose trended higher in the muscle of non-survivors, making more carbohydrate available for glycolytic and TCA processing. Indirect evidence presented for the liver, both at baseline and shock, supports the hypothesis that non-survivors process more carbohydrate than do survivors. Two TCA cycle intermediates, fumarate (0.98) and succinate (0.93), trended higher in pigs that died, further supporting the hypothesis of increased TCA cycle activity in the muscle of non-survivors. The greater oxygen extraction ratio observed in non-survivors adds support for the higher rate of ATP production rather than diminished ATP demand at baseline (**Supplemental Table 2**).

ATP can be produced through mechanisms other than carbohydrate supply to the TCA cycle. Upon de-amination, amino acids can enter the TCA cycle. Non-survivors exhibited higher levels

of the three branched-chain amino acids (and 3-hydroxyisovalerate) in the muscle. This observation was accompanied by a higher level of urea (arising from the deamination process) in the serum of non-survivors ($p=0.09$). Unique to muscle is the ability to generate ATP from CrP. The level of CrP trended higher in non-survivors but was not differentiating. The reader is referred to the Baseline Urine Results for additional information on possible contributions of CrP to muscle ATP production.

Serum: *The level of glycerol was lower in non-survivors. Amino acid and urea levels support the hypothesis of enhanced proteolysis and/or elevated biosynthesis in non-survivors.*

Serum glucose (0.43) and lactate (0.25) levels did not differentiate outcomes. Levels of the branched-chain amino acids (>1), as well as the isoleucine catabolite 3-methyl-2-oxovalerate (1.39), were higher in the serum of animals that died. Serum levels of several other amino acids [arginine, glycine, histidine, phenylalanine, proline, serine, threonine (all >1) and tyrosine (0.75)], as well as urea ($p=0.09$, Supplemental **Table 1c**), were also higher and mostly differentiating in animals that died compared to those that lived. The levels of glycerol (1.08), acetoacetate (1.58) and β -hydroxybutyrate (0.62) were lower in non-survivors. ATP is not visible in the serum.

The level of glucose did not differentiate outcomes. Indirect evidence suggests that non-survivors differed in their glucose processing. Randal's widely accepted glucose-fatty acid cycle states that glucose provision promotes glucose use and decreases reliance on fats as fuel and vice versa³⁶. Since we did not perform extraction of lipids, glycerol was evaluated as a surrogate marker for lipolysis. Non-survivors exhibited a lower level of glycerol suggesting that the degree of lipolysis was lower in these animals. We offer this observation as support for the premise that non-survivors metabolize a greater amount of glucose or have a greater ability to process glucose than survivors.

One of the notable observations at this time point was the higher level of amino acids in the serum of non-survivors relative to survivors. Free amino acids arise from: 1) the digestion of dietary protein; 2) proteolysis of endogenous proteins; 3) biosynthesis. It is unlikely that the higher levels of amino acids in non-survivors can be attributed to elevated digestion since the ingested food source is carbohydrate. Proteolysis of endogenous proteins is a likely possibility for the elevated levels of amino acids in non-survivors. Higher levels of the serum-observable essential amino acids (amino acids that cannot be synthesized *de novo*) phenylalanine, histidine, and threonine point to greater protein breakdown in non-survivors. The higher levels of branched-chain amino acids (also essential amino acids) in the muscle of non-survivors correlate with these serum observations.

The resulting free amino acids can serve as precursors for various biological molecules. Phenylalanine is a building block for tyrosine, which is a precursor to, for example, adrenaline and thyroxine. Histidine is a precursor for formiminoglutamate, which can be transferred to tetrahydrofuran, a major carrier of 1-carbon units for biosynthesis. Serine serves as the carbon skeleton for glycine, which is a building block for multiple biological entities including proteins, purines, and collagen. Both serine and glycine levels were higher in the serum of non-survivors. Both arginine and urea are products of the urea cycle; levels of both were greater in non-survivors. As indicated in Muscle Results; this higher level of serum urea in non-survivors could also have arisen from elevated catabolism of branched-chain amino acids for fuel. Therefore, the higher levels of free amino acids observed in non-survivors are likely a result of elevated proteolysis as well as biosynthesis.

Urine: *Fuel sources did not separate outcome groups. Higher levels of catabolic products in the urine of non-survivors represent a major class of differentiating metabolites.*

Levels of urine glucose (0.49) and lactate (0.59) were not differentiating between outcomes. Branched-chain amino acids were not NMR-visible in the urine. The level of tryptophan (1.40) was lower, while the levels of tyrosine (1.02) and glycine (1.04) were higher in non-survivors (see below). The level of acetoacetate (0.19) did not separate survivors from non-survivors. ATP was not NMR-visible in the urine.

The level of niacinamide (2.94) was higher in the urine of animals that died, suggesting greater catabolism of tryptophan in non-survivors. The trends in the levels of tryptophan and niacinamide observed in the urine of non-survivors are in agreement with the NAD^+ trend suggested in the muscle of animals that died (see above).

Catabolic products of tyrosine and histidine were observed in urine. Tyrosine is enzymatically decarboxylated to form tyramine. The level of tyramine (1.27) was higher in the urine of animals that died and reflected the serum pattern of tyrosine. Excess histidine is enzymatically converted to urocanate. The level of uroconate (2.73) was higher in the urine of animals that died and reflected the histidine patterns observed in the serum.

The creatinine level was higher in the urine of non-survivors by ~50% (0.46). Creatinine arises from the spontaneous cyclization of creatine during the generation of ATP from CrP in tissues that contain CrP, notably muscle. Migrating to the blood, creatinine is excreted in the urine. N-methylhydantoin is formed during the bacterial degradation of creatinine in the gut³⁷. The level of N-methylhydantoin was higher in the urine of animals that died compared to those that lived (1.48). The higher levels of urine creatinine and N-methylhydantoin correlate with the higher level of muscle ATP in animals that died. These observations support the concept that the higher level of ATP in the muscle of non-survivors can be partially attributed to greater use of CrP for

ATP production. However, the level of creatinine was lower in the serum of non-survivors suggesting, alternatively, that the rate of creatinine excretion is greater in non-survivors. An accelerated rate of creatinine excretion has been reported following a protein meal³⁸. Digestion of the protein would result in an increase in serum amino acids similar to the situation observed in non-survivors and represents a potential explanation for the increased rate of creatinine clearance.

Trimethylamine (1.83) and trimethylamine N-oxide (1.44) levels were lower in the urine of animals that died compared to those that lived. Both trimethylamine and trimethylamine N-oxide serve to counteract the protein-destabilizing effects of urea in the kidney³⁹. With higher levels of urea observed in the serum of non-survivors, it seems logical that higher levels of these amines would have been required to mitigate the effects of elevated urea. Thus these higher levels would have been observed in the urine. To resolve this discrepancy, additional work would be needed to determine the rate of trimethylamine N-oxide production as well as accumulation in tissues. In accordance with our findings in muscle and serum, the metabolic profile in urine suggests increased protein turnover in pigs that died.

Oxygen Physiology:

There was a trend toward greater oxygen extraction ($p = 0.07$) and lower venous oxygen saturation in non-survivors ($p = 0.12$) (**Supplemental Table 2**).

3.4 Shock Interval (Fig 7)

Data refer to the changes in levels of metabolites observed during the shock interval compared to baseline (S45-B). Two animals died during this time period, dropping the total non-surviving sampling set from 15 at baseline to 13 animals at the end of the shock period **Fig. 2**.

Liver: *Greater increases in the levels of liver glucose and branched-chain amino acids were observed in non-survivors when compared to survivors. The level of the vasodilator adenosine increased to a greater extent in animals that died.*

In liver during the shock phase, both outcome groups exhibited an increase in the level of glucose. The increase in glucose (1.14) in animals that died was greater by more than 50% compared to those that lived. The change in the level of lactate (1.26) reflects this pattern. The levels of branched-chain amino acids (>1.70) increased in both groups with the increase being greater in non-survivors. Other amino acids exhibited varying trends and levels of significance (see below). The increase in the level of β -hydroxybutyrate (0.80) was higher in non-survivors by approximately 4-fold. Both surviving and non-surviving animals exhibited a decrease in the level of ATP (0.30).

With shock, hormones are released that mobilize glycogen stores. The greater increase in the level of glucose observable in the liver of non-survivors during shock suggests that more glycogen is broken down with the advent of shock in animals that died. As outlined in the Baseline Results for the liver, following a carbohydrate pre-feed glucose enters the cell and is converted to G6P. The lower levels of liver ATP and pentose phosphate pathway products at baseline suggest that glycogen production is preferentially operational at baseline in non-survivors resulting in more glucose released during shock.

The level of tyrosine (1.60) increased to a greater extent in non-survivors. Tyrosine is a precursor to the catecholamines, which are part of the physiologic response to hemorrhagic shock and trauma⁴⁰.

The level of GSH (1.01) increased to a greater extent (~4-fold) in non-survivors. The level of methionine (1.43), a GSH precursor, increased in non-survivors but decreased in survivors. The level of NAD⁺ (1.45) increased in pigs that died with almost no change observed in survivors. The level of NADP⁺ (1.93) increased in pigs that died but decreased in pigs that lived. These trends suggest that increased activities in the pathways that produce these metabolites (e.g. the pentose phosphate pathway) are a component of the inherent stress response. When observed at baseline, levels of these markers were higher in survivors. Thus, the liver in survivors could be predisposed to a beneficial and/or protective metabolism prior to the initiation of shock and trauma.

Degradation of ATP is a known occurrence during ischemic events^{41,42}. To facilitate the need for increased oxygen, the ATP-degradation intermediate AMP can be converted to the vasodilator adenosine⁴³. AMP that is not diverted to the production of adenosine can be further degraded to hypoxanthine (**Fig. 6**) The increase in the level of adenosine (1.26) observed in animals that died was approximately 3 times greater than the increase seen in animals that lived. Animals that died also exhibited an increase in the level of hypoxanthine (1.60) compared to baseline while animals that lived exhibited the opposite trend. These observations suggest that non-survivors altered metabolism to meet the demand for vasodilation to a greater extent than did survivors. Also noteworthy is that pigs that died exhibited a higher increase in arginine (0.78), which is a precursor for the vasodilator NO. The lower DO₂ (**Supplemental Table 2**) recorded during shock in non-survivors would be a strong physiologic signal for increased vasodilation.

Muscle: *Animals that died exhibited a greater decrease in the level of ATP compared to animals that lived; this occurred despite a greater turnover in CrP in non-surviving animals.*

The level of muscle glucose increased to approximately the same degree (0.29) in both outcome groups but the increase in the level of lactate (1.87) was approximately 3.5 fold higher in non-

surviving animals compared to surviving animals. Branched-chain amino acid (>0.9) levels increased in both outcome groups but the increase was smaller for animals that died. The level of 3-hydroxyisovalarate [leucine catabolite (2.07)] increased in survivors but decreased in non-survivors. Animals that died exhibited a small decrease in the level of β -hydroxybutyrate (1.60) at S45 compared to baseline; animals that survived exhibited a small increase. CrP strongly differentiated survivors from non-survivors. Both groups exhibited a drop in the level of CrP (2.24) compared to baseline, but the drop in animals that died was over 5-fold greater than that recorded for animals that lived. The level of ATP (1.26) increased in animals that lived but decreased in animals that died.

A greater increase in the level of lactate characterizes non-survivors relative to survivors. An increase in the level of lactate is indicative of a hypoxic environment. The accompanying oxygen data (**Supplemental Table 2**) and the observed elevated liver adenosine support the hypothesis that non-survivors experience diminished oxygen available. Additionally, there was increased reliance on oxygen-independent generation of ATP. Termed substrate level phosphorylation, ATP is formed by direct transfer of a phosphate group from, for example, CrP or succinyl-CoA to the corresponding purine diphosphate⁴⁴. The decrease in the level of muscle CrP from baseline in animals that died is over 5-fold higher than that recorded for animals that lived. The increase in the level of muscle succinate (arising from the actions of succinate thiokinase on succinyl CoA) in animals that died was double that observed in survivors (**Fig. 7**). A similar succinate increase was observed in the serum. Despite these efforts the level of ATP dropped in the muscle of non-survivors suggesting that demand is greater than production capacity.

Serum: *The level of glucose increased during shock in both outcome groups. Higher levels of succinate, lactate, and adenosine were associated with animals that died.*

The increase in the level of glucose (0.46) from baseline to S45 was higher in non-survivors relative to survivors but not differentiating. The increase in the lactate level (1.23) in non-surviving animals was approximately 1.5 times greater than that observed in surviving animals. The levels of branched-chain amino acids increased (<1) in animals that lived and decreased in animals that died. Other amino acids exhibited varying patterns with those patterns being strongly differentiating for glutamate (2.41), glycine (1.08), and histidine (1.0). Both outcome groups saw an increase in the level of urea ($p=0.24$) over baseline. While the change in the level of acetoacetate (0.02) was not discriminating, the increase in the level of β -hydroxybutyrate (1.13) was greater in animals that died. The increase in the level of glycerol (1.94) over baseline in non-surviving animals was nearly double that observed in surviving animals.

Succinate (2.08) strongly differentiated non-survivors from survivors. Animals that died exhibited approximately a 2.5 -fold greater increase over baseline compared to animals that lived. Lactate exhibited a similar trend. Both serum metabolites mirrored the pattern of higher

levels of succinate and lactate observed in the muscle of non-survivors. Adenosine (1.82) and hypoxanthine (1.67) levels increased over baseline to a greater extent in animals that died compared to those that lived. The trend in adenosine and hypoxanthine levels in the serum paralleled those seen in the liver.

Urine: *During hemorrhage, animals minimize fluid loss. Consequently, urine volumes were reduced and metabolite information largely reflected baseline observations.*

Note: Because urine is normalized to urine output (cc/hr/kg) which decreases during shock, urine metabolite data are the means at shock rather than the differences between S45 and Baseline. The levels of glucose (0.54) and lactate (0.21) did not differentiate outcomes, but the level of the glucose-derived sugar mannose (1.79) was higher in the urine of animals that died. The level of acetoacetate (0.81) was not differentiating between outcomes.

The patterns in glycine (1.48), trimethylamine N-oxide (1.63), tyramine (1.44), and urocanate (1.66) observed at Baseline persisted at the shock time point. The level of methylguanidine (1.47), which accumulates in the urine during uremia, was higher in animals that died. This information suggests that animals that die are unable to counteract the effects of the incremental increase in protein catabolism at the shock time point.

The level of 1-methylnicotinamide (2.11) was lower in animals that died relative to those that survived. Urinary 1-methylnicotinamide excretion is reflective of renal blood flow with a lower level suggestive of diminished flow⁴⁵. The levels of hypoxanthine (2.14) and xanthine (1.53) were both higher in animals that died. This pattern suggests that non-survivors experience higher levels of purine degradation relative to those that survived.

Oxygen Physiology:

After shock induction, oxygen consumption (VO_2) dropped in animals that died, with no change observed in survivors (**Supplemental Table 2**). Additional oxygen data suggest that this decrease is a direct consequence of changes in the ability to oxygenate. Importantly, animals that die experience a greater rate of lung injury with an earlier onset. Acute lung injury (ALI) is commonly defined as a $\text{PaO}_2:\text{FiO}_2$ ratio (P:F ratio) <300 , while a P:F ratio <200 marks acute respiratory distress syndrome (ARDS). The average P:F ratio in non-survivors was significantly lower at the end of the shock period ($p=0.04$), with two animals experiencing ALI. In contrast, animals that lived did not show changes in lung function at this time point.

3.5 Early Resuscitation

Data refer to the changes in metabolite levels observed during the early resuscitation period compared to the shock interval (FR2-S45). Seven animals died during this interval, dropping the

total non-surviving sampling set from 15 at baseline to 6 animals at the end of early resuscitation (Fig. 2).

Liver: Levels of several fuel sources mobilized during shock decreased in both outcome groups; lactate increased in non-survivors but decreased in survivors.

In both outcome groups, the level of glucose (0.17) decreased. The level of lactate (2.22) increased in non-survivors but decreased in survivors. The levels of branched-chain amino acids (≤ 0.6) decreased in both groups, while β -hydroxybutyrate (0.76) levels increased. The level of ATP (0.12) rebounded to a small extent in both outcome groups. However, the level of AMP (1.76) decreased in non-survivors but increased in survivors. The level of adenosine (0.57) dropped in both outcome groups.

Muscle: Levels of fuel sources mobilized during shock in the muscle decreased in both outcome groups with the exception of valine. Lactate and succinate levels increased to a greater extent in non-survivors.

The level of glucose (0.13) decreased in both outcome groups. The level of lactate (1.31) increased in non-survivors while decreasing in survivors. Levels of leucine and isoleucine (≤ 0.35) increased to a minor extent, while the level of valine (1.12) increased in survivors but decreased in non-survivors. Both outcome groups exhibited an increase in the level of β -hydroxybutyrate (0.10). The level of CrP (0.72) decreased in both survivors and non-survivors. The level of ATP (1.57) dropped in both outcome groups but the decline in non-survivors was approximately 4-fold that observed in survivors.

The level of succinate (0.95) increased to a greater extent in non-survivors. The higher level of succinate suggests that substrate level phosphorylation evident during the shock interval is still operational during early resuscitation in non-survivors. However, this alternate cycling mode did not result in an increase an ATP level similar to that observed in survivors.

Serum: Levels of NMR-visible fuel sources decreased in both outcome groups with the exception of glycerol in non-survivors. Multiple other metabolites differentiated outcomes but trends varied.

The level of glucose (0.42) declined in both outcome groups. The level of lactate (1.38) decreased in both groups but to a lesser extent in pigs that died. The decreases in serum levels of branched-chain amino acids (~ 1.0) and β -hydroxybutyrate (0.85) were greater in non-survivors. The level of glycerol (1.38) continued to increase in non-survivors but decreased in survivors.

Twenty of the 47 identified metabolites in the serum exhibited a VIP score above 1 with variable patterns. This high number of differentiating variables probably reflects the effect of hemorrhage

and trauma on multiple tissues as well as unique physiologic timetables. Adenosine (0.86) and succinate levels (0.18) declined in both outcome groups to nearly the same extent.

Urine: Previously mobilized fuel sources were evident in the urine. The level of allantoin was higher in non-survivors.

Note: Because urine is normalized to urine output (cc/hr/kg), urine metabolite data are the means at FR2 rather than the differences between FR2 and S45.

The level of glucose (0.94) observed in non-survivors was nearly double that seen in survivors during early resuscitation. Additionally, the level in each outcome group represented the highest concentration of glucose recorded for any of the sampling time points. The level of lactate (1.17) followed a similar pattern with the level in non-survivors being 2-fold greater than that seen in survivors. The levels of two other glucose-derived sugars, mannitol (1.32) and mannose (1.25) were higher in non-survivors. The level of acetoacetate (0.10) did not separate outcomes.

The level of allantoin (1.24) was greater in the urine of non-survivors. Allantoin arises from the processing of uric acid, a downstream intermediate in purine degradation (**Fig. 6**). When xanthine dehydrogenase acts on xanthine, it generates uric acid as the primary product. If xanthine oxidase acts on xanthine, hydrogen peroxide and uric acid are generated. Uric acid can be then be converted to allantoin that gets excreted in the urine. In humans allantoin is formed when reactive oxygen species (ROS) act on uric acid and allantoin is considered a marker of oxidative stress in humans⁴⁶. Xanthine oxidase is also present in pig tissue⁴⁷ and the oxidizing environment it generates represents a possible route for the production of allantoin. However, pigs also have uricase, an enzyme that converts uric acid into allantoin. The higher level of allantoin in non-survivors suggests that conversion of available purine intermediates to the end product (allantoin) is higher in non-survivors. This study did not provide information on the activity of either xanthine oxidase or uricase. Additionally, the level of hypoxanthine (1.78), a uric acid precursor, was lower in non-survivors, but the level of xanthine (0.18), the subsequent precursor to uric acid, was approximately the same in both outcome groups. Thus, the explanation for the elevated level of allantoin in non-survivors requires further investigation.

The levels of phenylalanine (1.78) and its downstream metabolite tyrosine (0.75) were higher in the urine of non-survivors. Tyrosine can be enzymatically decarboxylated to form tyramine (1.56), the level of which was higher in the urine of non-survivors. This pattern of metabolites invites investigation into the requirement for and production rate of norepinephrine and epinephrine, especially during the shock phase.

In a situation similar to that observed in the serum, there are multiple metabolites (23/61) that exhibit a VIP score above 1. The large number of VIP metabolites greater than 1 probably

reflects the effect of hemorrhage and trauma across the entire organism as well as the timing of individual responses.

Oxygen physiology

After two hours of full resuscitation, 67% (4/6) of non-survivors experienced ALI or ARDS, compared to 24% (4/17) in survivors (**Supplemental Table 2**).

4.0 Discussion

With this work we have examined metabolic profiles in the liver, muscle, serum, and urine of pre-fed animals during before, during, and after hemorrhagic shock with trauma. As hypothesized, these profiles differentiated non-survivors from survivors. Our data suggest that, although all animals are subjected to the same experimental protocol, non-survivors exhibit altered carbohydrate processing as early as the baseline sampling point. This could be the consequence of a larger quantity of ingested pre-feed (unintended consequences of oral delivery) or the result of a greater innate ability to process carbohydrates. In this discussion we establish a relationship between altered carbohydrate processing and two potential mechanisms of death: formation of the mitochondrial permeability transition pore and mitigation of protective mechanism associated with fasting.

4.1 Mitochondrial Permeability Transition Pore

The basis for our study was earlier work that indicated pre-feeding reduces the death rate in animal models of hemorrhagic shock. The death rate for pre-fed animals in our study was nearly double that of fasted animals (47% vs 28%). Unlike these earlier studies, our protocol did include resuscitation. The majority of pre-fed deaths occurred following resuscitation¹⁰ and strongly suggest ischemia/reperfusion injury (I/R)⁴⁸⁻⁵⁰. Formation of the mitochondrial permeability transition pore (mPTP) is currently considered an important contributor to I/R death. The mPTP is an opening that occurs in the inner mitochondrial membrane. Its formation enables passage of small molecules and fluid into and out of the mitochondria. Recent studies suggest that opening of the mPTP can be transient (termed flickering). In this scenario, opening contributes to cell homeostasis. Prolonged opening with the accompanying loss of membrane potential leads to compromised ATP formation, exacerbated ROS production, matrix swelling and potential cell death. The probability that a cell will survive has been inversely correlated with the percentage of cellular mitochondria that undergo mPTP formation. The contemporary working model recognizes that numerous factors can influence the probability of mPTP opening by modulating the threshold for formation^{51, 52}.

4.1.1 Electron Transport Chain Complex I Activity as a Threshold-modulating Agent for mPTP Formation

The mitochondrial electron transport chain is composed of four protein complexes called complex I, II, III, and IV. TCA cycle metabolism of carbohydrates (glucose and deaminated amino acids) favors supply of electrons to complex I by virtue of an elevated NADH:FADH₂ ratio. Complete catabolism of fats generates more FADH₂, thus decreasing the NADH:FADH₂ ratio relative to carbohydrate metabolism and favoring production of ATP with greater reliance on complex II. Increased activity of complex I, independent of other known modulators such as ROS, has been associated with increased probability of mPTP formation and gradient collapse⁵³⁻⁵⁵.

At Baseline the level of ATP was greater in the muscle of non-survivors. Greater production of ATP in this outcome group correlated with a greater oxygen extraction ratio at baseline in animals that died. A review of the fuel sources indicates that non-survivors exhibited a greater level of glucose as well as higher levels of branched-chain amino acids at Baseline in the muscle. Although β -oxidation was not determined in the muscle, the level of serum glycerol (surrogate for lipolysis) was lower in animals that died. This profile suggests that glucose and deaminated amino acids are the primary feed for the TCA cycle in non-survivors. The resulting higher ratio of NADH:FADH₂ preferentially sends electrons through complex I of the electron transport chain, lowering the threshold for formation of mPTP. Thus entering the shock phase, non-survivors were already biased toward opening of the mPTP¹². The advent of shock mobilizes more glucose and results in additional flux through complex I, increasing the likelihood of extended mPTP opening with the ensuing consequences of membrane collapse and/or matrix swelling^{53,56}. This scenario is a possible explanation for the mismatch between ATP demand and the ability to produce ATP observed in muscle during the shock phase.

A generally accepted model of I/R injury contends that ischemia itself does not cause mPTP formation, but rather creates the conditions for opening upon reperfusion⁵². However, a study on human microvascular endothelial cells cultured in high glucose conditions reported the advent of release of cytochrome c and cell death⁵⁵. Release of cytochrome c is considered a marker of mPTP formation. Tharakan provides evidence of cytochrome c release from the mesentery tissue in a rat model of hemorrhagic shock prior to resuscitation. Opening of the mPTP in the vasculature is associated with loss of junctional integrity^{57,58}. Although we did not study the vasculature, a higher degree of mPTP induction in the vasculature of non-survivors is a possible explanation for the significantly lower P:F ratio observed in non-survivors at the end of the shock period.

4.1.2 Reactive Oxygen Species as a Threshold-modulating Agent for mPTP Formation

For a given flux of electrons through the electron transport chain, activity of complex I generates more ROS than operation of complex II. Additionally, when respiring on succinate, isolated

mitochondria have been shown to exhibit reverse electron flow. When reverse electron flow occurs, electrons travel from complex II to complex I rather than the expected complex III. This reverse flow is associated with a high rate of superoxide production at complex I^{59, 60}. Increased levels of serum succinate have been observed during hypoxic events⁴³, likely leading to an increase in ROS. The initial increase in the level of ROS may serve as a trigger for an additional ROS burst. This phenomenon is termed ROS-induced ROS release and can propagate to neighboring mitochondria resulting in further damage⁵¹. Increased oxidative stress reduces the threshold for opening of the mPTP⁶¹⁻⁶³.

We postulated above (4.1.1) that non-survivors processed more fuel through (muscle) complex I at baseline. Non-survivors also had higher levels of glucose in the serum available for processing through complex I in the tissues at shock. Succinate levels increased to a greater extent in the liver and muscle in non-survivors at shock, increasing the probability of reverse electron flow. These observations support the possibility of greater ROS generation in non-survivors, favoring the opening of the mPTP. Although we have no direct measurement of ROS, non-survivors did exhibit a higher level of allantoin, a potential marker of oxidative stress, in the urine at the end of the resuscitation sampling point.

One of the targets of ROS oxidation is the set of critical dithiols at discrete sites within the mitochondrial pore. Under normal circumstances endogenous antioxidants such as glutathione mitigate potential mitochondrial damage. In non-survivors the level of GSH was lower in the liver at baseline. We hypothesized that this arose from reduced pentose phosphate pathway activity in the liver of non-survivors. As a result, these animals had a lower level of an antioxidant defense mechanism entering the shock phase. Although non-survivors showed higher increases in GSH and other pentose phosphate pathway substrates during the shock interval, it is possible that this shift occurred too late to mitigate the initial ROS damage and the subsequent ROS-induced ROS release. Oxidation of these critical dithiol sites has been shown to lower the threshold for mPTP opening^{64, 65}.

4.1.3 Increase in the Mitochondrial Calcium Level as a Threshold-modulating Agent for mPTP Formation

Other examples of altered carbohydrate processing are the greater increases in the levels of lactate observed in the liver, muscle, and serum of non-survivors during shock. One of the compensating mechanisms to normalize intracellular acidosis is activation of the Na^+/H^+ exchanger. Operation of this exchanger moves H^+ out of the cell that is countered by Na^+ movement into the cell. This leads to accumulation of sodium within the cell. Under non-pathological conditions, the Na^+/K^+ -ATPase pump functions to remove excess intracellular sodium. In an ischemic environment its function is compromised. To compensate for the still-elevated levels of intracellular Na^+ , the $\text{Na}^+/\text{Ca}^{2+}$ exchanger operates in reverse mode. Reversal of

normal operation of this exchanger coupled with reduction in Ca^{2+} uptake into the sarcoplasmic reticulum and a reduction in Ca^{2+} efflux via the sarcolemmal Ca^{2+} pump results in cytosolic calcium overload. Increased Ca^{2+} in the cytosol eventually increases mitochondrial Ca^{2+} ^{66, 67}. An increased calcium level lowers the threshold for mPTP opening ^{52, 62}.

4.2 Carbohydrate Pre-feed Mitigates the Protective Effects of Fasting

As indicated from our earlier work ¹⁰ the death rate for fasted animals was approximately half that observed for pre-fed animals. Food deprivation initiates physiologic adaptations designed to use internal fuel reserves. A study in rat gastrocnemius muscle indicated that the transition to use of stored fats can be observed within 12 hours following the initiation of the fast ⁶⁸. As discussed above, β -oxidation of fatty acids generates more FADH_2 than when carbohydrates alone provide electron donors for the electron transport chain. This increase in the flow of electrons to complex II reduces the probability of mPTP formation that is associated with complex I activity ⁶⁹. Recent work has also documented that the physiologic response to food deprivation and the response initiated to ensure survival following stress/trauma share multiple pathways ⁷⁰⁻⁷³.

An overnight fast has been shown to deplete glycogen reserves in fasted animals and agrees with the schedule for the implementation of fatty acid metabolism ^{68, 74}. Since we did not investigate lipids, we have only indirect evidence that fatty acids were being metabolized to a greater extent in survivors when compared to non-survivors. The level of serum glycerol (our surrogate marker for lipolysis) was higher in survivors when compared to non-survivors at baseline. Thus, survivors have a greater probability of active stress-protection pathways relative to survivors when shock/trauma was initiated.

We believe that fruitful areas of future investigation could focus on metformin or cyclosporine A, compounds that have been shown to affect the activity of complex I and mPTP opening ⁷⁵. Treatment with cyclosporine A (or an alternative inhibitor of mPTP) may improve survival after shock and resuscitation in pre-fed pigs. ⁷⁶⁻⁷⁸ Also, if differences in carbohydrate processing decrease the threshold for mPTP opening, treatment with stable isotope-labeled nutrients can give enhanced insight into carbohydrate processing before and after induction of trauma and hemorrhage. In addition, a particularly interesting aspect that arose in this analysis is the significantly decreased P:F ratio in non-survivors at the end of the shock period. This observation invites future investigation into the role of mPTP opening in changes in vascular integrity and differences in extravascular fluid movements in hemorrhagic shock and trauma. Interestingly, cyclosporine A pre-treatment alleviated shock-induced vascular hyperpermeability in rats ⁵⁸. Other studies showed improved vasoreactivity and hemodynamics after cyclosporine A treatment in rat models of hemorrhagic shock. ^{76, 78}

5. Conclusions

Carbohydrate pre-feed prior to hemorrhagic shock with injury resulted in a death rate approaching 50%. We used our metabolomic analysis of the liver, muscle, serum, and urine to propose a hypothesis that describes the metabolism associated with death in these animals: non-survivors experienced altered carbohydrate processing when compared to survivors. As a result of this scenario, we have identified three factors in non-survivors (greater flux thru electron transport chain complex I, a higher level of ROS and elevated Ca^{2+} quantities) that increase the probability of mPTP opening. Mitochondrial insults are cumulative and the chance of multiple mitochondria accruing sufficient signals to initiate mPTP opening increases with each added factor. Loss of fasting-associated activation of protective pathways also represents a potential explanation for the higher death rate.

There are limitations to this study. The scope of the data revealed other differences between outcomes that are not discussed in this paper. For example, lactate dehydrogenase was already higher at baseline in animals that died (data not shown). Future work should include a control group that has no or minimal surgical preparation prior to shock/ trauma induction to investigate the effect of pre-shock surgical preparation. Not all metabolites were visible in each compartment. Tissue metabolites can reside in different intracellular locations; our tissue preparation method did not allow for any such identification. Lipid analysis was not performed. We also recognize that the complexity of biological systems renders any interpretation of this data open to debate. In keeping with this possibility, we invite further exploration of our data (<http://www.ebi.ac.uk/metabolights/MTBLS123>). Our work joins the body of literature that shows hyperglycemia prior to an ischemic event is associated with morbidity and dysfunction⁷⁹⁻⁸².

Acknowledgements: The authors wish to thank the Office of Naval Research for their continued funding of this research (grants N00014-09-1-0323 and N000-05-1-0344), the Minnesota Supercomputing Institute, the Minnesota NMR Center (funding for NMR instrumentation was provided by the Office of the Vice President for Research, the Medical School, the College of Biological Science, NIH, NSF, and the Minnesota Medical Foundation), and the University of Minnesota.

Figure and Table Captions

Figure 1: Graphical Representation of Experimental Timeline.

Tissue and fluid sampling time points are shown in parentheses (B, S45, FR2). SBP, systolic blood pressure; Hbg, blood hemoglobin; UO, urine output.

Figure 2: Forty-eight Hour Survival in Fasted and Pre-fed Pigs after Polytrauma and Resuscitation.

There was a trend towards increased mortality in animals receiving a carbohydrate feed 60 minutes before surgery when compared to fasted animals (15/32 or 47% vs 9/32 or 28%, $p=0.153$). FR20, 20 hours after beginning of full resuscitation; PR24, 24 hours after end of full resuscitation. Figure modified from Colling et al., Shock, 2015¹⁰.

Figure 3: PLS-DA Scores Plots for the Shock Interval

PLS-DA scores plots show model discrimination between outcome groups during the response to shock in each of the four compartments (liver, muscle, serum, urine). Models are of varying quality and statistical significance as reported in Table 1. PC, principal component.

Figure 4: Heat Maps of Select Fuel Metabolites

4A: Heat maps highlight differences in fuel metabolites (liver, muscle, serum) for each time interval discussed, according to survival. This figure is meant to be a visual guide for the reader to quickly assess differences in fuel metabolites discussed at the beginning of each compartment's subsection in the results. Colors indicate the scaled increase or decrease in metabolite abundance. Baseline columns reflect the scaled abundance of the metabolite at baseline. Subsequent columns show the scaled increase or decrease in metabolite abundance. Red indicates an increase and blue indicates a decrease. BHB, β -hydroxybutyrate.

4B: Heatmaps highlight differences in significant urinary metabolites for each time point discussed, according to survival. Scaled metabolite abundances are shown in red, with darker shades of red indicating higher levels of the metabolite. Individual time points are shown instead of time intervals as in Figure 3A because urine metabolite levels are expressed in terms of hourly urine output (nanomoles of metabolite per hour per kg). TMAO, trimethylamine N-oxide.

Figure 5: Baseline Metabolite Profile Comparing Non-survivors to Survivors.

The level of muscle ATP, a downstream indicator of glucose provision, was greater in non-survivors. The level of formate, a 1-carbon unit involved in anabolic biosynthesis, was also higher in animals that died. Higher levels of branched-chain (BCAA) and other amino acids (AA) in the muscle and serum of non-survivors support the hypothesis of an elevated degree of proteolysis in animals that died. In the anabolic environment created by glucose provision, these amino acids can be used as building blocks for other amino acids. The level of glucose was differentiating and lower in the liver of non-survivors and is reflected in a lower level of ATP

level in pigs that died. In contrast to the muscle, the liver metabolite profile suggests that animals that died exhibited a lower degree of biosynthetic activity compared to animals that lived. This is evidenced by the lower levels of liver GSH, hypoxanthine (HX), AMP, NAD⁺ and NADP⁺ in non-survivors. All these metabolites arise from activity of the pentose phosphate pathway (PPP), the pathway involved in anabolic biosynthesis. The lower level of glycerol, our marker of lipid breakdown, in non-survivors suggests that the degree of lipolysis was lower in non-survivors at baseline. Various metabolites that reflect tissue patterns were observed in the serum and urine. OXPHOS, oxidative phosphorylation; TMA, trimethylamine.

+ = level of this metabolite was higher in non-survivors compared to survivors

- = level of this metabolite was lower in non-survivors compared to survivors

(+) = level of this metabolite was in higher in non-survivors compared to survivors with p= 0.09

Figure 6: ATP Degradation.

ADP and AMP are early stage products of ATP hydrolysis. During an ischemic event such as hemorrhagic shock, AMP can be hydrolyzed to provide the vasodilator adenosine⁴³. Alternatively, AMP degradation results in the production of hypoxanthine⁸³, which is further metabolized to xanthine and then uric acid by xanthine dehydrogenase (XDH) or xanthine oxidase (XO)⁸⁴. Additionally, in pigs, uric acid is also be converted to allantoin and H₂O₂ enzymatically by uricase. Both uric acid and allantoin are excreted in the urine. During biosynthesis, AMP can be generated from ribose 5-phosphate, a product of the pentose phosphate pathway. IMP, inosine monophosphate.

Figure 7: S45-B Metabolite Profile Comparing Non-survivors to Survivors

A closed arrow represents non-survivors; an open arrow represents survivors. Up arrows represent an increase in the level of metabolite compared to baseline; down arrows represent a decrease in the level of metabolite compared to baseline. Larger arrows signify greater changes in the designated group for metabolites with VIP>1.

Several fuel sources were mobilized to combat the effects of shock and injury. The level of muscle glucose increased over baseline in both groups but the change was not differentiating between outcomes. The level of lactate (lac) exhibited a similar increase but the increase from baseline was higher in non-survivors. The increase in muscle branched-chain amino acids was lower in non-survivors. The level of muscle ATP dropped from baseline in non-survivors despite a suggested increased use of creatine phosphate. The increase in the level of glucose was higher and differentiating in the liver of non-survivors and is hypothesized to arise from a greater degree of glycogen formation at baseline in non-survivors. Both outcome groups exhibited an

increase over baseline in the level of liver lactate, but the increase was higher in non-survivors. The glucose and lactate changes in pigs that died were accompanied by a shift to the biosynthetic pattern observed at baseline in survivors: non-survivors exhibited a greater increase when compared to baseline in the levels of methionine, GSH, NAD^+ , and NADP^+ . Metabolic products from tissue processes were observed in the serum and urine. The more substantial increase in the serum succinate level over baseline in non-survivors represents a potential biomarker of shock mortality.

Table 1: PLS-DA Model Diagnostics

Diagnostics for PLS-DA models were constructed for each physiological compartment and each time point or time interval discussed. Diagnostics reported are: R^2 (indicative of the predictive utility of the model), NMC (indicative of the number of samples misclassified as lived or died and standard deviation), classification accuracy (indicative of the overall accuracy of sample classification as “lived” or “died”), and permutation p-value (indicative of model significance). Note that at baseline and shock, there is at least one PLS-DA model that shows a statistically significant difference between survival groups (permutation p-value<0.05).

Supplemental Figure and Table Captions

Supplemental Figure 1A: PLS-DA Scores Plots for Baseline

PLS-DA scores plots show model discrimination between outcome groups at Baseline in each of the four compartments (liver, muscle, serum, urine). Models are of varying quality and statistical significance as reported in Table 1. Note that at baseline and shock, there is at least one PLS-DA model that shows a statistically significant difference between survival groups (permutation p -value <0.05).

Supplemental Figure 1B: PLS-DA Scores Plots for Resuscitation Time Intervals.

PLS-DA scores plots show model discrimination between outcome groups during the response to shock (FR2-S45) in each of three compartments (liver, muscle, serum). As described in the text, urine models were analyzed at FR2 to reflect the normalization of the data to urine output. Models are of varying quality and statistical significance as reported in Table 1.

Supplemental Table 1: VIP Scores and Means

Tables S1A-D are each on a separate tab in the .xlsx worksheet. Baseline values represent means for each metabolite. Values for the subsequent time intervals (S45-B and FR2-S45) represent the mean difference. As discussed in the manuscript, urine values are reported at B, S45, and FR2 instead of at B, S45-B, and FR2-S45. Liver and muscle values are reported as mM/1 g lyophilized muscle tissue. Mean serum values are reported as mmol/L. Mean urine values are reported as nmol/hr/kg. Serum urea values were obtained from a Gem Premier 3000 blood gas analyzer (Instrumentation Laboratories, Chicago, IL) and means are reported in the table. Mann-Whitney U tests were performed to assess urea statistical significance between survival groups. At baseline, $p=0.09$; at S45-B, $p=0.2$; at FR2-S45 $p=0.04$.

Supplemental Table 2: Blood Oxygen Parameters.

Data is presented as median (interquartile range). DO_2 , delivered oxygen; ERO_2 , oxygen extraction ratio; PaO_2 , arterial partial pressure of oxygen; PvO_2 , venous partial pressure of oxygen; P:F ratio, PaO_2/FiO_2 ratio; VO_2 , systemic oxygen consumption; SvO_2 , mixed venous oxygen saturation. * $p<0.05$ in survivors versus non-survivors for the same time point/ interval. #As a marker of acute respiratory failure, P:F ratio was compared at single time points (B, S45, FR2), not time intervals.

References

- 1 B. J. Eastridge, R. L. Mabry, P. Seguin, J. Cantrell, T. Tops, P. Uribe, O. Mallett, T. Zubko, L. Oetjen-Gerdes, T. E. Rasmussen, F. K. Butler, R. S. Kotwal, J. B. Holcomb, C. Wade, H. Champion, M. Lawnick, L. Moores and L. H. Blackbourne, *J. Trauma. Acute Care. Surg.*, 2012, **73**, S431-7 (DOI:10.1097/TA.0b013e3182755dcc [doi]).
- 2 W. Xiao, M. N. Mindrinos, J. Seok, J. Cuschieri, A. G. Cuenca, H. Gao, D. L. Hayden, L. Hennessy, E. E. Moore, J. P. Minei, P. E. Bankey, J. L. Johnson, J. Sperry, A. B. Nathens, T. R. Billiar, M. A. West, B. H. Brownstein, P. H. Mason, H. V. Baker, C. C. Finnerty, M. G. Jeschke, M. C. Lopez, M. B. Klein, R. L. Gamelli, N. S. Gibran, B. Arnoldo, W. Xu, Y. Zhang, S. E. Calvano, G. P. McDonald-Smith, D. A. Schoenfeld, J. D. Storey, J. P. Cobb, H. S. Warren, L. L. Moldawer, D. N. Herndon, S. F. Lowry, R. V. Maier, R. W. Davis, R. G. Tompkins and Inflammation and Host Response to Injury Large-Scale Collaborative Research Program, *J. Exp. Med.*, 2011, **208**, 2581-2590 (DOI:10.1084/jem.20111354 [doi]).
- 3 W. A. Knaus, E. A. Draper, D. P. Wagner and J. E. Zimmerman, *Crit. Care Med.*, 1985, **13**, 818-829.
- 4 S. P. Baker, B. o'Neill, W. Haddon Jr and W. B. Long, *Journal of Trauma and Acute Care Surgery*, 1974, **14**, 187-196.
- 5 C. M. DUNHAM, J. H. SIEGEL, L. WEIRETER, M. FABIAN, S. GOODARZI, P. GUADALUPI, L. GETTINGS, S. E. LINBERG and T. C. VARY, *Crit. Care Med.*, 1991, **19**, 231-243.
- 6 D. P. MILZMAN, B. R. BOULANGER, A. RODRIGUEZ, C. A. SODERSTROM, K. A. MITCHELL and C. M. MAGNANT, *Journal of Trauma and Acute Care Surgery*, 1992, **32**, 236-244.
- 7 C. Nettelblatt, A. Alibegovic and O. Ljungqvist, *Nutrition*, 1996, **12**, v-699.
- 8 A. Alibegovic and O. Ljungqvist, *Circ. Shock*, 1993, **39**, 1-6.
- 9 O. Ljungqvist, E. Jansson and J. Ware, *Circ. Shock*, 1986, **22**, 251-260.
- 10 K. P. Colling, U. P. Iyegha, J. I. Asghar, D. R. Lexcen, E. R. Luszczek, C. E. Determan Jr, N. E. Witowski, K. E. Mulier and G. J. Beilman, *Shock (Augusta, Ga.)*, 2015, **44**, 103.
- 11 E. R. Luszczek, T. Vincent, D. Lexcen, V. Kulkarni, K. Mulier and G. Beilman, *BMC emergency medicine*, 2015, **15**, 13.
- 12 N. Witowski, E. Luszczek, C. Determan Jr, D. Lexcen, K. Mulier, B. Ostrowski and G. Beilman, 2015, .

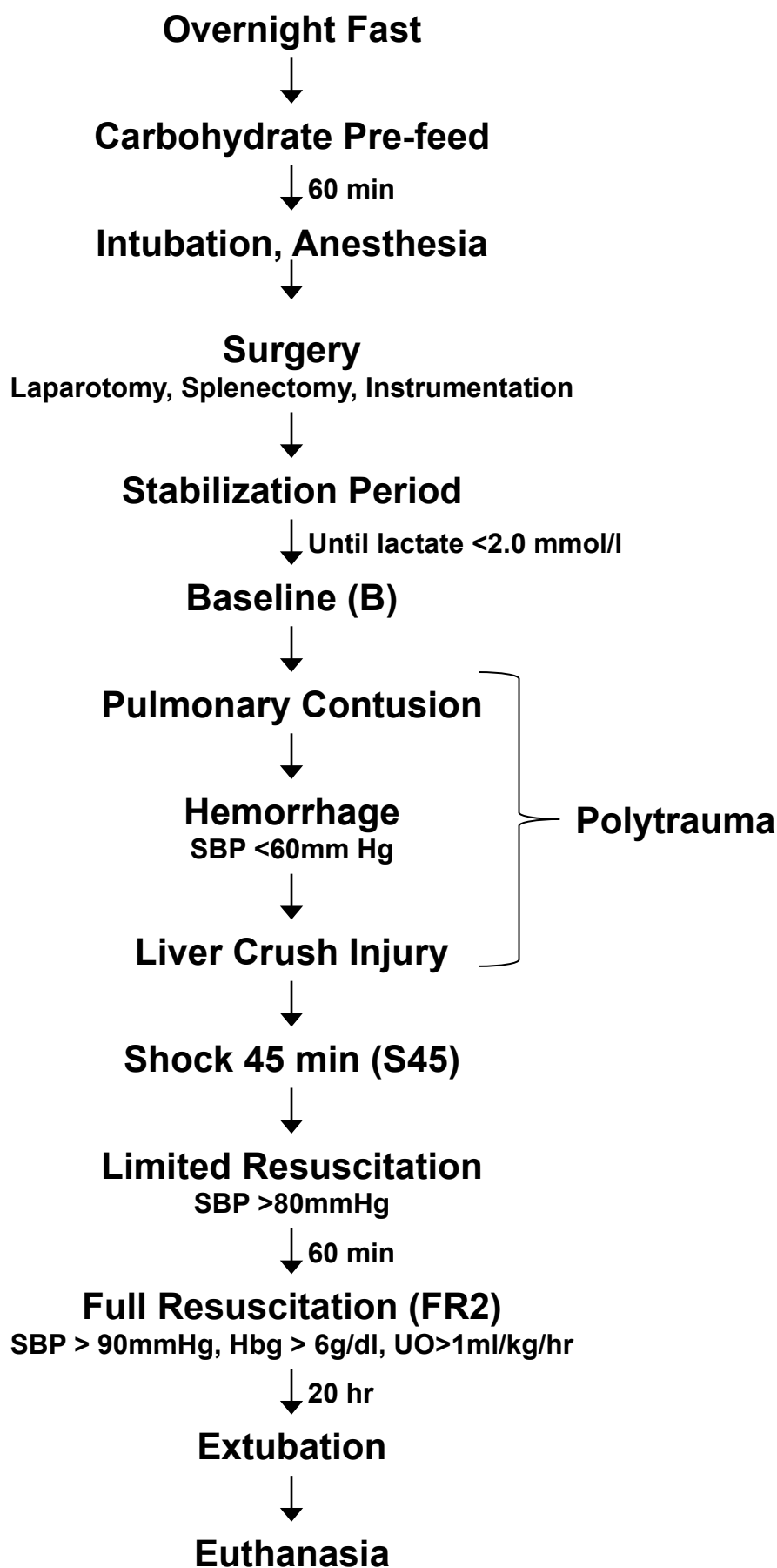
- 13 C. E. Determan Jr , E. R. Luszczyk, N. E. Witowski, D. Lexcen, K. E. Mulier and G. J. Beilman, *Metabolomics*, 2014, **10**, 950-957 (DOI:- 10.1007/s11306-014-0621-6).
- 14 K. E. Mulier, J. G. Greenberg and G. J. Beilman, *J. Surg. Res.*, 2012, **174**, e31-5.
- 15 K. E. Mulier, G. J. Beilman, M. J. Conroy, J. H. Taylor, D. E. Skarda and B. E. Hammer, *Shock*, 2005, **23**, 248-252.
- 16 J. B. Holcomb, A. E. Pusateri, R. A. Harris, T. J. Reid, L. D. Beall, J. R. Hess and M. J. MacPhee, *Journal of Trauma-Injury Infection & Critical Care*, 1999, **47**, 233-240.
- 17 M. A. Viant, in *Methods in Molecular Biology*, ed. W. Weckwerth, Humana Press, 2007, p. 229.
- 18 O. Beckonert, H. C. Keun, T. M. Ebbels, J. Bundy, E. Holmes, J. C. Lindon and J. K. Nicholson, *Nature Protocols*, 2007, **2**, 2692-2703.
- 19 R. J. Mortishire-Smith, G. L. Skiles, J. W. Lawrence, S. Spence, A. W. Nicholls, B. A. Johnson and J. K. Nicholson, *Chem. Res. Toxicol.*, 2004, **17**, 165-173.
- 20 A. M. Weljie, J. Newton, P. Mercier, E. Carlson and C. M. Slupsky, *Anal. Chem.*, 2006, **78**, 4430-4442.
- 21 E. Luszczyk, T. Nelson, D. Lexcen, K. Mulier, N. Witowski and G. Beilman, *Journal of Bioanalysis & Biomedicine*, 2011, **3**, 38 (DOI:10.4172/1948-593X.1000041).
- 22 R Foundation for statistical computing, Vienna, Austria, , <http://www.R-project.org/>, 2013.
- 23 S. Bijlsma, I. Bobeldijk, E. R. Verheij, R. Ramaker, S. Kochhar, I. A. Macdonald, B. van Ommen and A. K. Smilde, *Anal. Chem.*, 2006, **78**, 567-574.
- 24 J. Trygg, E. Holmes and T. Lundstedt, *Journal of proteome research*, 2007, **6**, 469-479.
- 25 K. H. Liland, *TrAC Trends in Analytical Chemistry*, 2011, **30**, 827-841.
- 26 D. R. Lexcen, E. R. Luszczyk, N. E. Witowski, K. E. Mulier and G. J. Beilman, *The Journal of Trauma and Acute Care Surgery*, 2012, **73**, S147-55.
- 27 E. R. Luszczyk, D. R. Lexcen, N. E. Witowski, K. E. Mulier and G. Beilman, *Metabolomics*, 2013, **9**, 223-235.
- 28 Sanchez G, *Tools of the trade for discriminant analysis.*, **Error! Hyperlink reference not valid.**, 2012.

- 29 G. Simpson, *permute: Functions for generating restricted permutations of data. R package version 0.7-0 [internet]*, <http://CRAN.R-project.org/package=permute>, 2012.
- 30 E. Szymańska, E. Saccenti, A. K. Smilde and J. A. Westerhuis, *Metabolomics*, 2012, **8**, 3-16.
- 31 M. A. Orman, I. P. Androulakis, F. Berthiaume and M. G. Ierapetritou, *J. Theor. Biol.*, 2012, **293**, 101-110.
- 32 K. Heininger, *Int. Rev. Neurobiol.*, 2002, **51**, 103-158.
- 33 J. G. Salway, *Metabolism at a Glance*, John Wiley & Sons, 2013.
- 34 K. L. McIntire, Y. Chen, S. Sood and R. Rabkin, *Kidney Int.*, 2014, **85**, 374-382.
- 35 J. C. Anthony, T. G. Anthony, S. R. Kimball and L. S. Jefferson, *J. Nutr.*, 2001, **131**, 856S-860S.
- 36 K. N. Frayn, *Biochem. Soc. Trans.*, 2003, **31**, 1115-1119 (DOI:10.1042/ [doi]).
- 37 M. Wyss and R. Kaddurah-Daouk, *Physiol. Rev.*, 2000, **80**, 1107-1213.
- 38 S. Tam, L. Tang, C. Lai, M. Nicholls and R. Swaminathan, *Clin. Sci.*, 1990, **78**, 481-485.
- 39 G. N. Somero, *Physiology*, 1986, **1**, 9-12.
- 40 M. M. Meguid, M. F. Brennan, T. T. Aoki, W. A. Muller, M. R. Ball and F. D. Moore, *Archives of Surgery*, 1974, **109**, 776-783.
- 41 E. Koustova, P. Rhee, T. Hancock, H. Chen, R. Inocencio, A. Jaskille, W. Hanes, C. R. Valeri and H. B. Alam, *Surgery*, 2003, **134**, 267-274.
- 42 J. H. Taylor, G. J. Beilman, M. J. Conroy, K. E. Mulier and B. E. Hammer, *Journal of Trauma and Acute Care Surgery*, 2004, **56**, 251-258.
- 43 A. Deussen, V. Ohanyan, A. Jannasch, L. Yin and W. Chilian, *J. Mol. Cell. Cardiol.*, 2012, **52**, 794-801.
- 44 C. Chinopoulos, *Journal of Neuroscience Research*, 2013, **91**, 1030 (DOI:10.1002/jnr.23196).
- 45 C. Musfeld, J. Biollaz, N. Bélaz, U. W. Kesselring and L. A. Decosterd, *J. Pharm. Biomed. Anal.*, 2001, **24**, 391-404.
- 46 M. S. Plank, T. C. Calderon, Y. Asmerom, D. S. Boskovic and D. M. Angeles, *J. Vis. Exp.*, 2011, **(54)**. pii: 2948. doi, 10.3791/2948 (DOI:10.3791/2948 [doi]).

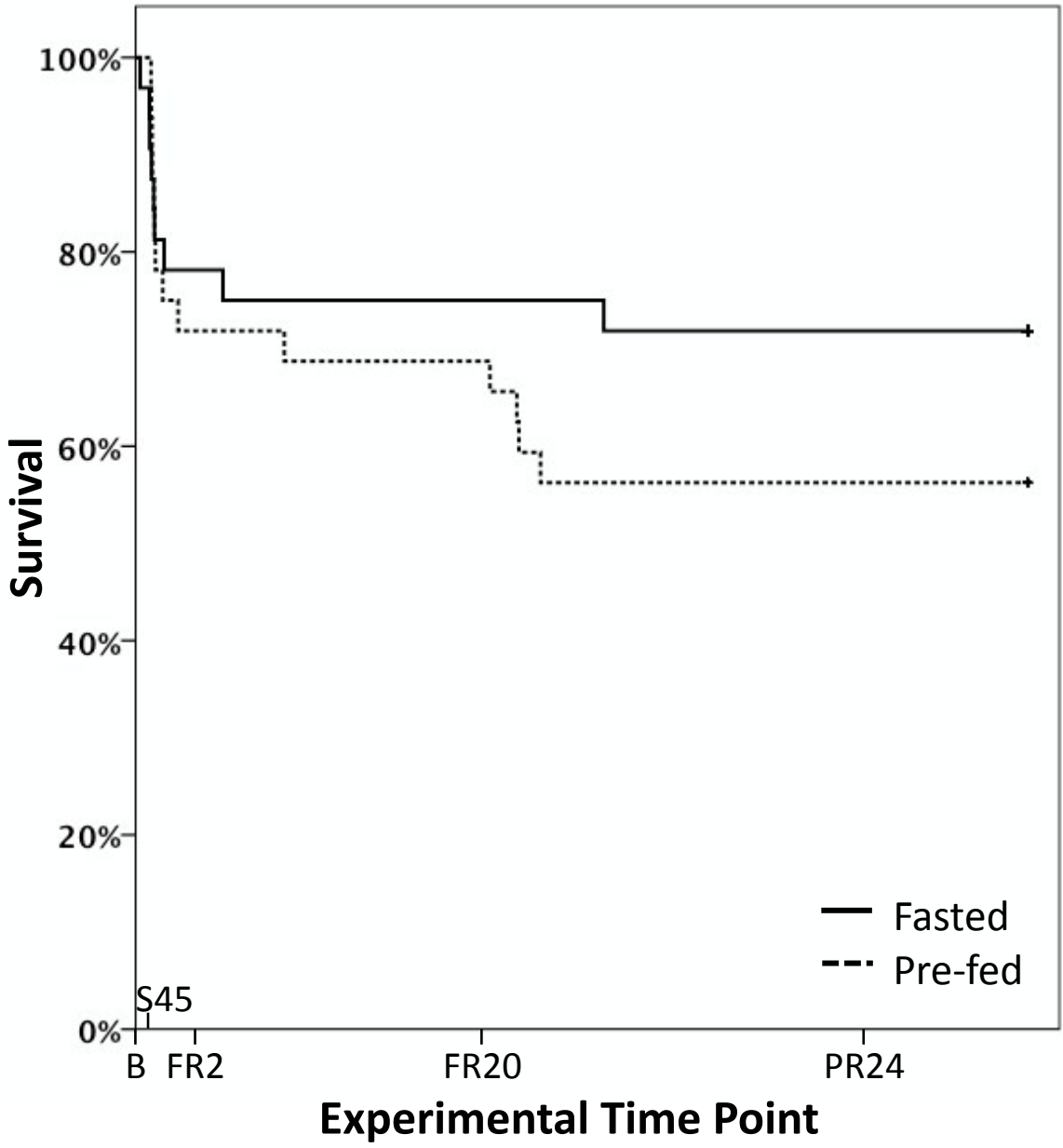
- 47 A. Dement'ev, *Russian agricultural sciences*, 2013, **39**, 82-85.
- 48 H. P. Santry and H. B. Alam, *Shock*, 2010, **33**, 229-241 (DOI:10.1097/SHK.0b013e3181c30f0c [doi]).
- 49 G. D. Rushing and L. D. Britt, *Ann. Surg.*, 2008, **247**, 929-937 (DOI:10.1097/SLA.0b013e31816757f7 [doi]).
- 50 H. M. Honda, P. Korge and J. N. Weiss, *Ann. N. Y. Acad. Sci.*, 2005, **1047**, 248-258.
- 51 D. B. Zorov, M. Juhaszova, Y. Yaniv, H. B. Nuss, S. Wang and S. J. Sollott, *Cardiovasc. Res.*, 2009, **83**, 213-225 (DOI:10.1093/cvr/cvp151 [doi]).
- 52 A. Rasola and P. Bernardi, *Cell Calcium*, 2011, **50**, 222-233.
- 53 E. Fontaine, O. Eriksson, F. Ichas and P. Bernardi, *J. Biol. Chem.*, 1998, **273**, 12662-12668.
- 54 P. Bernardi, A. Krauskopf, E. Basso, V. Petronilli, E. Blalchy-Dyson, F. Di Lisa and M. A. Forte, *Febs Journal*, 2006, **273**, 2077-2099.
- 55 D. Detaille, B. Guigas, C. Chauvin, C. Batandier, E. Fontaine, N. Wiernsperger and X. Leverve, *Diabetes*, 2005, **54**, 2179-2187 (DOI:54/7/2179 [pii]).
- 56 A. M. Porcelli, A. Angelin, A. Ghelli, E. Mariani, A. Martinuzzi, V. Carelli, V. Petronilli, P. Bernardi and M. Rugolo, *J. Biol. Chem.*, 2009, **284**, 2045-2052 (DOI:10.1074/jbc.M807321200 [doi]).
- 57 B. Tharakan, F. A. Hunter, W. R. Smythe and E. W. Childs, *Clinical and Experimental Pharmacology and Physiology*, 2010, **37**, 939-944.
- 58 B. Tharakan, J. G. Holder-Haynes, F. A. Hunter, W. R. Smythe and E. W. Childs, *J. Trauma*, 2009, **66**, 1033-1039 (DOI:10.1097/TA.0b013e31816c905f [doi]).
- 59 Y. Liu, G. Fiskum and D. Schubert, *J. Neurochem.*, 2002, **80**, 780-787.
- 60 A. Lambert and M. Brand, *Biochem. J.*, 2004, **382**, 511-517.
- 61 D. B. Zorov, M. Juhaszova and S. J. Sollott, *Physiol. Rev.*, 2014, **94**, 909-950 (DOI:10.1152/physrev.00026.2013 [doi]).
- 62 J. J. Lemasters, T. P. Theruvath, Z. Zhong and A. Nieminen, *Biochimica et Biophysica Acta (BBA)-Bioenergetics*, 2009, **1787**, 1395-1401.
- 63 F. Di Lisa, M. Canton, A. Carpi, N. Kaludercic, R. Menabò, S. Menazza and M. Semenzato, *Antioxidants & redox signaling*, 2011, **14**, 881-891.

- 64 P. Costantini, R. Colonna and P. Bernardi, *Biochimica et Biophysica Acta (BBA)-Bioenergetics*, 1998, **1365**, 385-392.
- 65 P. Costantini, B. V. Chernyak, V. Petronilli and P. Bernardi, *J. Biol. Chem.*, 1996, **271**, 6746-6751.
- 66 D. Garcia-Dorado, M. Ruiz-Meana, J. Inserte, A. Rodriguez-Sinovas and H. M. Piper, *Cardiovasc. Res.*, 2012, **94**, 168-180 (DOI:10.1093/cvr/cvs116 [doi]).
- 67 J. Inserte, J. A. Barrabes, V. Hernando and D. Garcia-Dorado, *Cardiovasc. Res.*, 2009, **83**, 169-178 (DOI:10.1093/cvr/cvp109 [doi]).
- 68 P. de Lange, P. Farina, M. Moreno, M. Ragni, A. Lombardi, E. Silvestri, L. Burrone, A. Lanni and F. Goglia, *FASEB Journal*, 2006, **20**, 2579-2581.
- 69 Z. V. Niatetskaya, S. A. Sosunov, D. Matsiukevich, I. V. Utkina-Sosunova, V. I. Ratner, A. A. Starkov and V. S. Ten, *J. Neurosci.*, 2012, **32**, 3235-3244 (DOI:10.1523/JNEUROSCI.6303-11.2012 [doi]).
- 70 J. S. Allard, L. K. Heilbronn, C. Smith, N. D. Hunt, D. K. Ingram, E. Ravussin and R. De Cabo, *PLoS One*, 2008, **3**, e3211.
- 71 S. P. Kunuthur, M. M. Mocanu, B. A. Hemmings, D. J. Hausenloy and D. M. Yellon, *J. Cell. Mol. Med.*, 2012, **16**, 1739-1749.
- 72 R. M. Anderson and R. Weindruch, *Trends in Endocrinology & Metabolism*, 2010, **21**, 134-141.
- 73 M. M. Sung, C. M. Soltys, G. Masson, J. J. Boisvenue and J. R. Dyck, *Journal of molecular medicine*, 2011, **89**, 291-302.
- 74 O. Ljungqvist, P. Boija, H. Esahili, M. Larsson and J. Ware, *American Journal of Physiology-Endocrinology And Metabolism*, 1990, **259**, E692-E698.
- 75 B. Brunmair, K. Staniek, F. Gras, N. Scharf, A. Althaym, R. Clara, M. Roden, E. Gnaiger, H. Nohl, W. Waldhausl and C. Fornsinn, *Diabetes*, 2004, **53**, 1052-1059.
- 76 Y. Lei, X. Peng, L. Liu, Z. Dong and T. Li, *J. Surg. Res.*, 2015, **195**, 529-540.
- 77 K. Kim, J. H. Shin, J. H. Lee, Y. H. Jo, M. A. Kim, K. Lee, K. W. Kang and Y. Hong, *Journal of Trauma and Acute Care Surgery*, 2015, **78**, 370-377.

- 78 D. Altavilla, A. Saitta, S. Guarini, M. Galeano, G. Squadrito, L. B. Santamaria, F. S. Venuti, C. Bazzani, A. Bertolini and F. Squadrito, *Cardiovasc. Res.*, 2001, **52**, 143-152 (DOI:S0008636301003625 [pii]).
- 79 R. Marfella, M. D'amico, C. Di Filippo, E. Piegari, F. Nappo, K. Esposito, L. Berrino, F. Rossi and D. Giugliano, *Diabetologia*, 2002, **45**, 1172-1181.
- 80 D. Nagamizo, S. Tsuruta, M. Matsumoto, H. Matayoshi, A. Yamashita and T. Sakabe, *Anesth. Analg.*, 2007, **105**, 1397-403, table of contents (DOI:105/5/1397 [pii]).
- 81 R. Hirose, F. Xu, K. Dang, T. Liu, M. Behrends, P. R. Brakeman, J. Wiener-Kronish and C. U. Niemann, *Anesthesiology*, 2008, **108**, 402-414 (DOI:10.1097/ALN.0b013e318164cff8 [doi]).
- 82 A. Blasi-Ibanez, R. Hirose, J. Feiner, C. Freise, P. G. Stock, J. P. Roberts and C. U. Niemann, *Anesthesiology*, 2009, **110**, 333-341 (DOI:10.1097/ALN.0b013e318194ca8a [doi]).
- 83 D. N. Granger, *Am. J. Physiol.*, 1988, **255**, H1269-75.
- 84 W. B. Poss, T. P. Huecksteadt, P. C. Panus, B. A. Freeman and J. R. Hoidal, *Am. J. Physiol.*, 1996, **270**, L941-6.

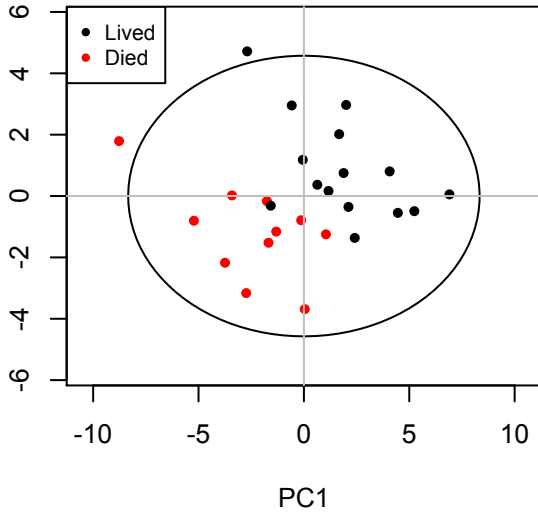


Kaplan- Meier Survival Plot

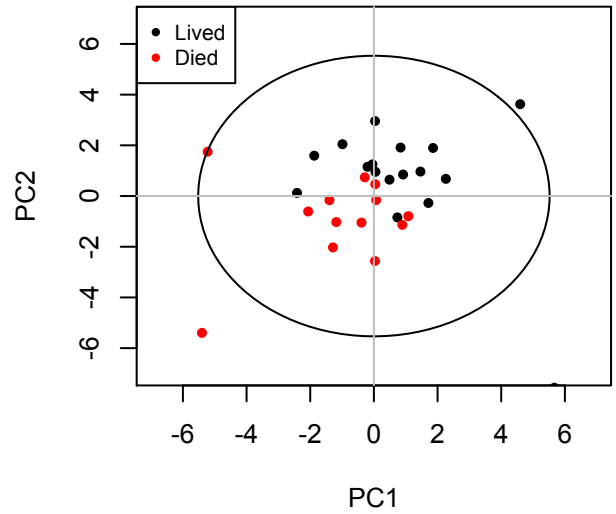


Molecular BioSystems Accepted Manuscript

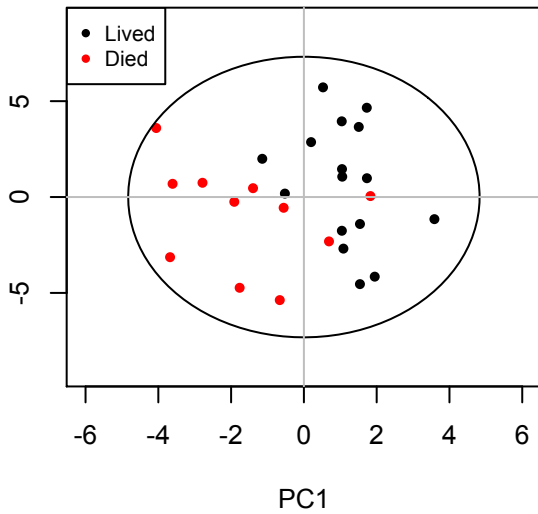
Liver S45-B



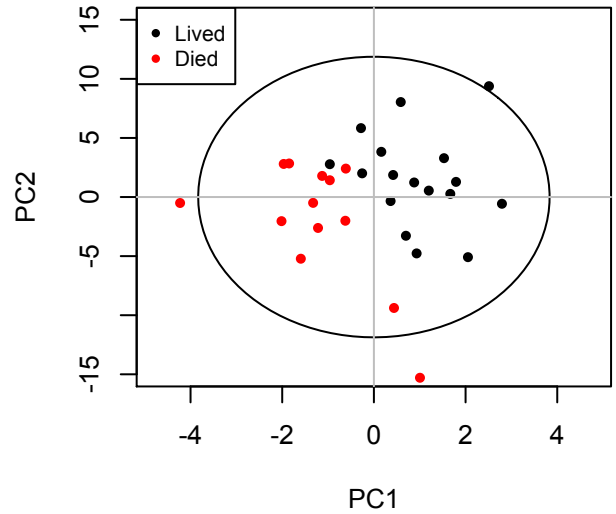
Muscle S45-B



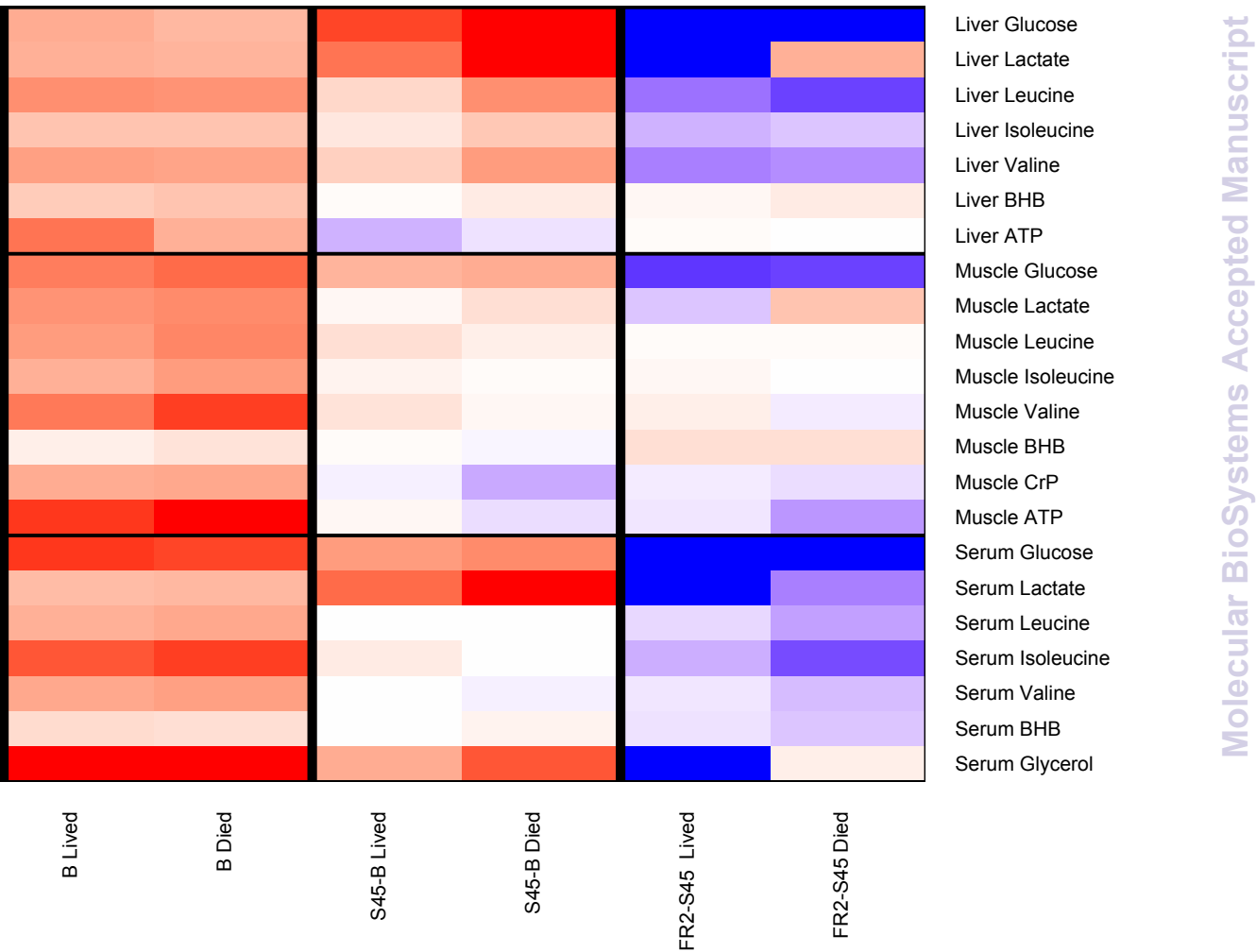
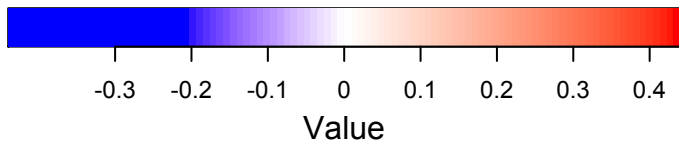
Serum S45-B

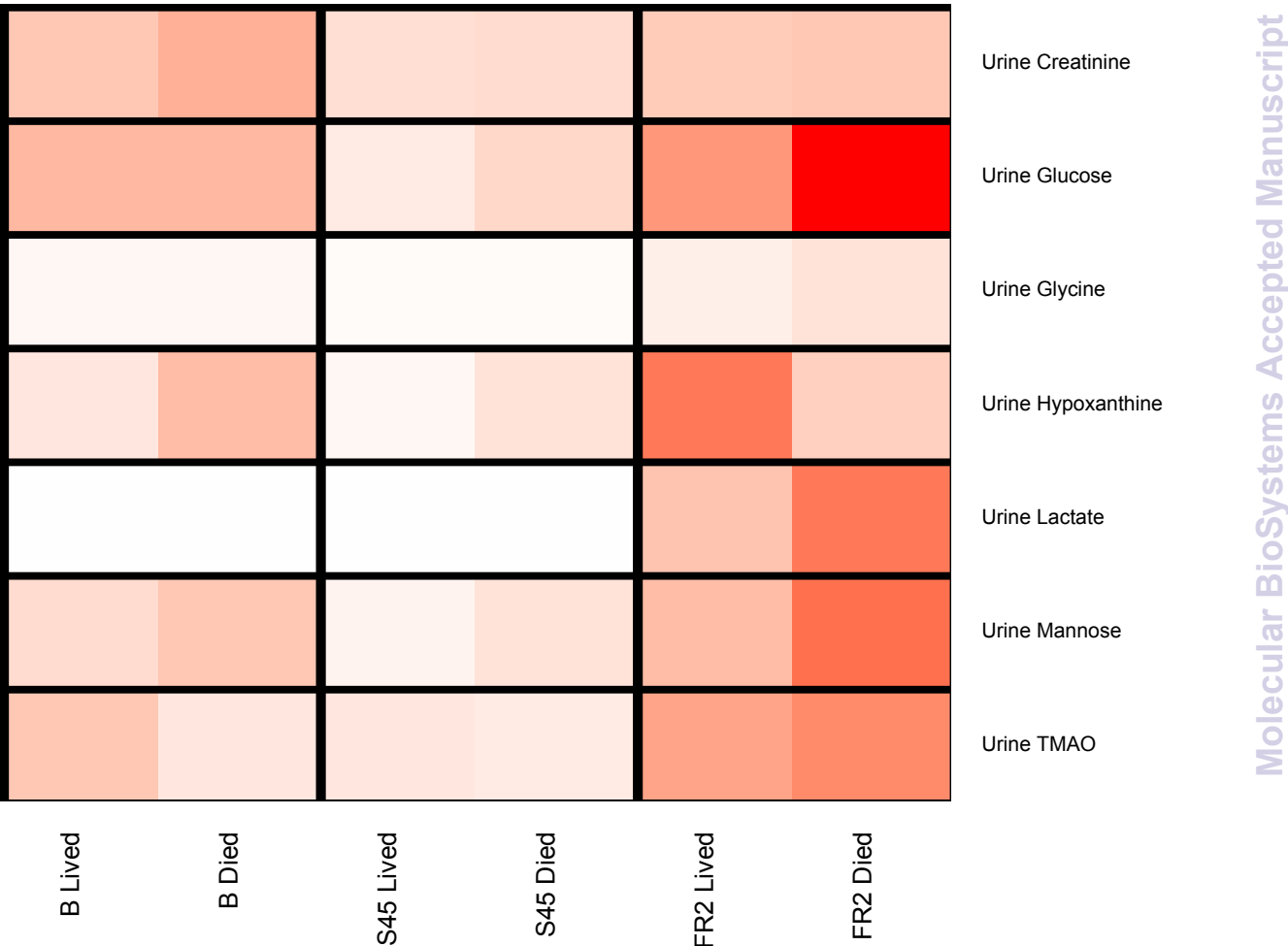
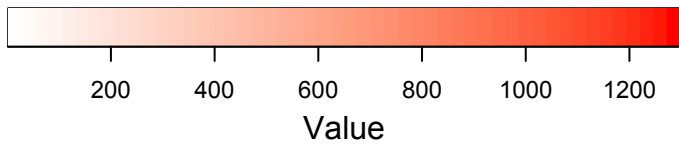


Urine S45

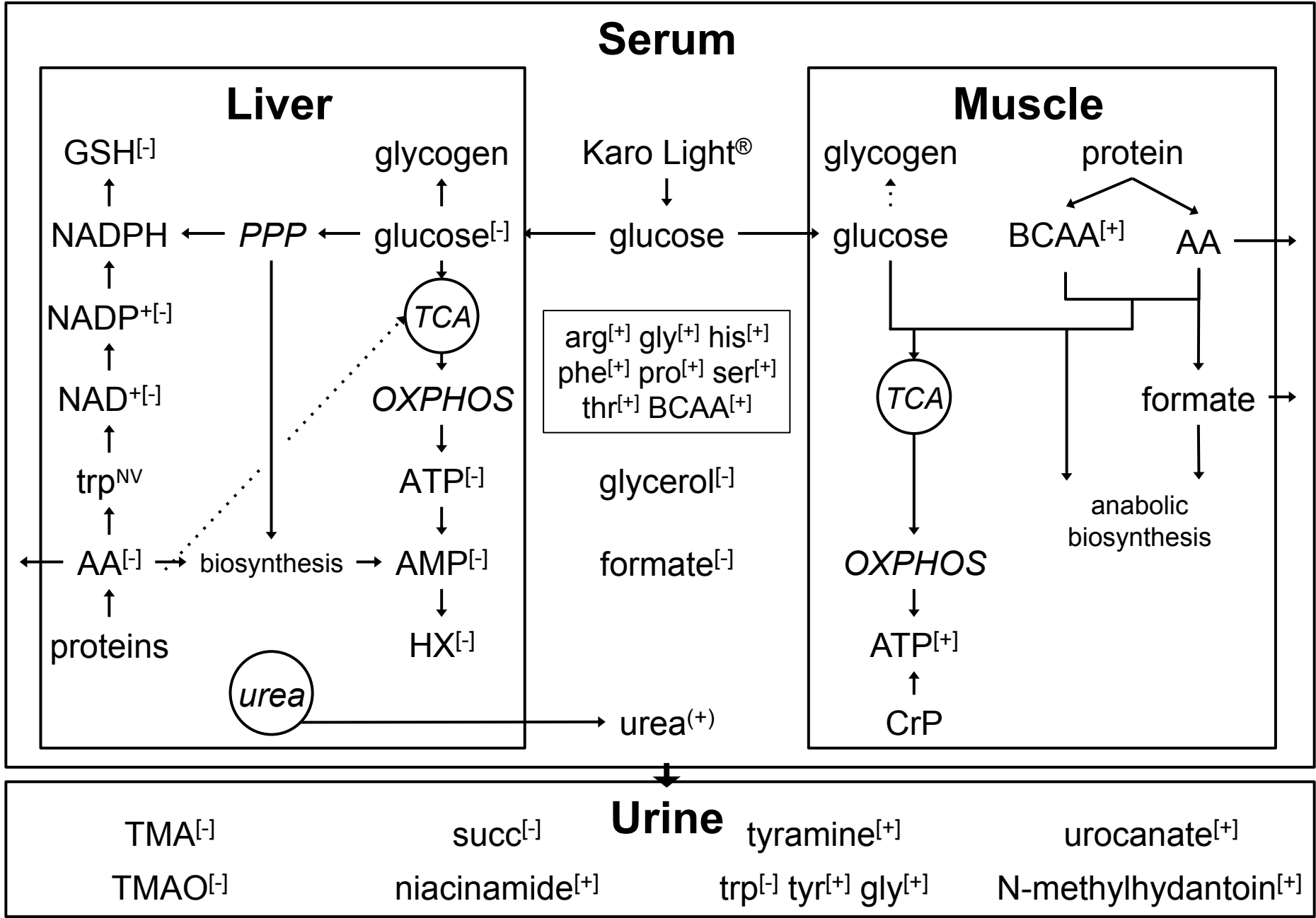


Color Key Molecular BioSystems

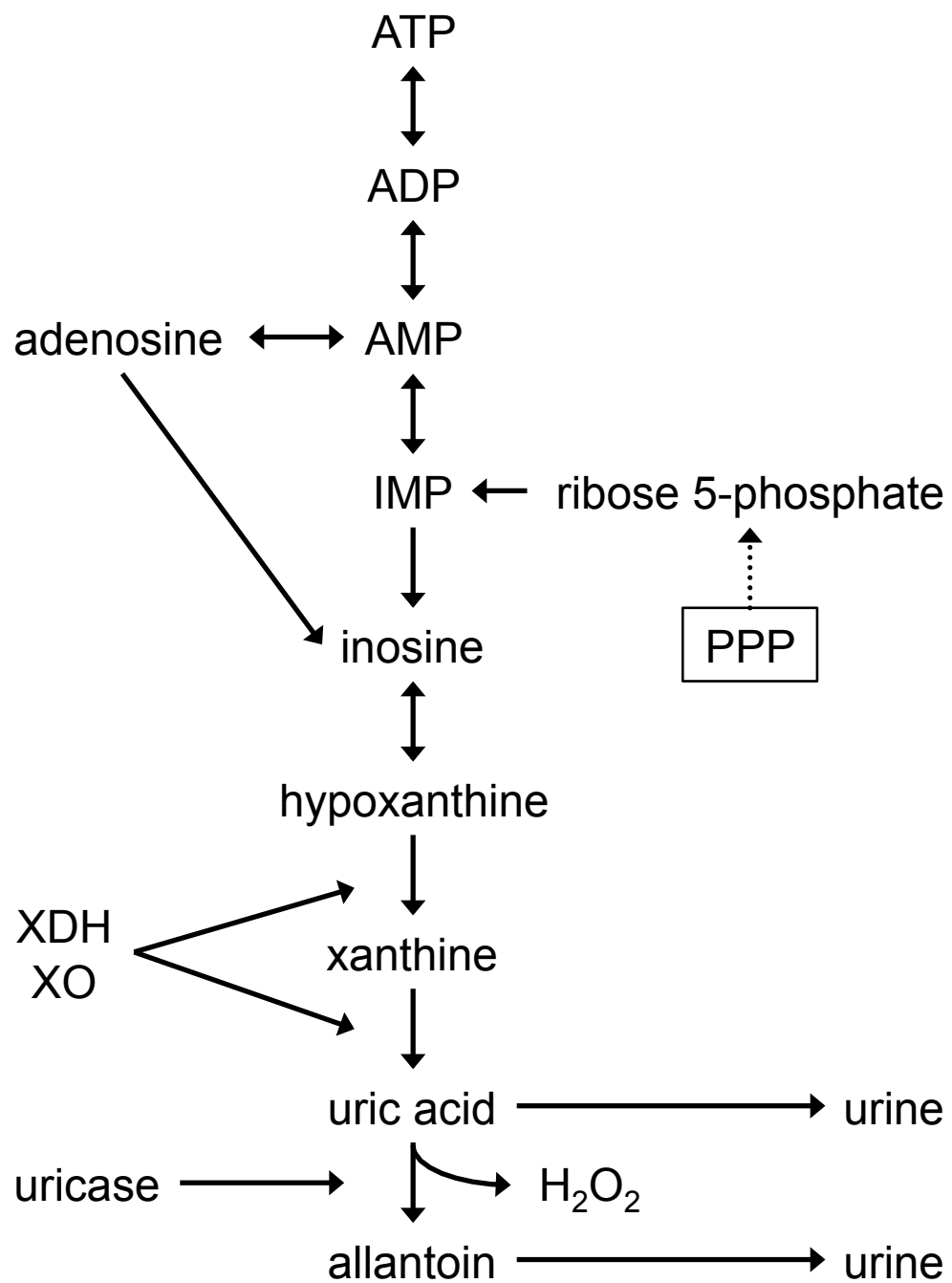




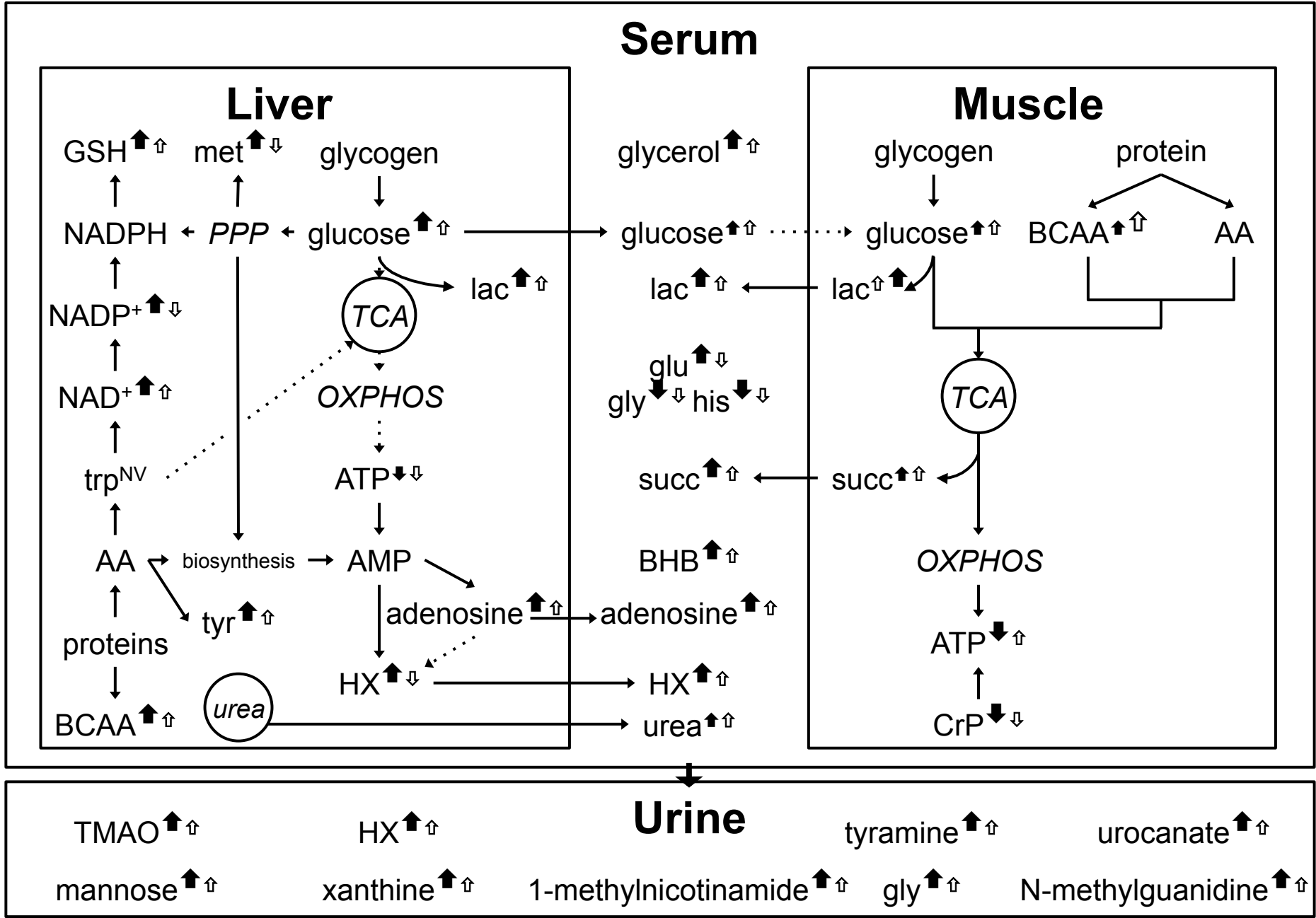
Pigs at baseline: lived versus died



Molecular BioSystems Accepted Manuscript



Pigs during shock: lived versus died



Molecular BioSystems Accepted Manuscript

Lived vs. Died

Compartment	Model	R ²	NMC ± std. dev.	Classification Accuracy	Permutation p-value
Liver	B	0.546	1.80 ±1.04	89.3%	0.926
	S45-B	0.703	1.23±0.88	92.3%	0.703
	FR2-S45	0.775	1.41±0.73	100%	0.10
Muscle	B	0.518	3.59±1.26	81.3%	0.957
	S45-B	0.361	3.30±1.17	83.3%	0.988
	FR2-S45	0.326	2.13±0.92	100%	0.108
Serum	B	0.592	3.29±1.16	96.8 %	0.06
	S45-B	0.564	1.29±0.95	96.3%	0.322
	FR2-S45	0.716	1.20±0.91	100%	0.163
Urine	B	0.555	2.96±1.26	96.9%	0.027
	S45	0.631	2.81±1.18	90%	0.01
	FR2	0.539	1.08±0.92	90.9%	0.933